NATIONAL ADVISORY COMMITTEE FOR AERONAUTICS

TECHNICAL NOTE 4037

STABILITY OF LAMINAR BOUNDARY LAYER NEAR A STAGNATION POINT OVER AN IMPERMEABLE WALL AND A WALL COOLED BY NORMAL FLUID INJECTION

By Morris Morduchow, Richard G. Grape,
and Richard P. Shaw

Polytechnic Institute of Brooklyn

Washington
August 1957

N

NATIONAL ADVISORY COMMITTEE FOR AERONAUTI

TECHNICAL NOTE 4037

STABILITY OF LAMINAR BOUNDARY LAYER NEAR A STAGNATION POINT OVER AN IMPERMEABLE WALL AND A WALL COOLED BY NORMAL FLUID INJECTION

By Morris Morduchow, Richard G. Grape, and Richard P. Shaw

SUMMARY

Minimum critical Reynolds numbers for laminar instability of two-dimensional stagnation flows over a wall cooled by normal fluid injection are determined theoretically. The individual as well as the net effects of wall temperature and normal fluid injection on the stability characteristics of the laminar boundary layer are thereby investigated. In order to study the effect of the favorable pressure gradient in this type of flow, comparison is made between results of calculations obtained herein and results of similar calculations for the flow over a flat plate. A comparison of various stability criteria is included, and, for certain cases of normal mass-flow injection, a slight appropriate extension in the approximate stability criteria is made.

A particularly interesting result obtained here is that, at fixed zero or low rates of fluid injection, the stabilizing effect of cooling of the wall is much greater for the flow over a flat plate than for the stagnation flows. In fact, over a highly cooled wall with zero or low rates of injection, the stagnation flows were found to have a minimum critical Reynolds number based on momentum thickness lower than that of the corresponding flat-plate flows.

INTRODUCTION

The purpose of this study is to investigate theoretically the stability of the laminar boundary layer in flow with an axial pressure gradient over a wall cooled by normal fluid injection. In particular, the separate as well as the simultaneous or net effects of wall temperature, of a small normal mass flow at the wall, and of a pressure gradient on the stability characteristics are determined. Such an investigation is of practical interest in connection with, for example, the transpiration, or sweat cooling, of rocket walls, turbine blades, and airfoils. A study

of the stability of the laminar boundary layer is of practical interest since, at least under conditions of a low free-stream turbulence, instability of the laminar boundary layer appears to be a necessary condition for transition to turbulence. The main advantages of maintaining a laminar boundary layer under these conditions would be a relatively low skin friction (provided that separation does not occur, cf. ref. 1) and a relatively low required normal mass flow of the coolant to maintain a given wall temperature.

The simultaneous effect of cooling of the wall and of a small normal mass flow at the wall is of especial interest, since the separate effects tend to oppose each other. In particular, lowering the wall temperature tends, by itself, to stabilize the laminar boundary layer, while a normal mass flow at the wall has, by itself, a destabilizing effect. It is therefore significant to determine under which conditions and to what extent the net effect of transpiration cooling is stabilizing or destabilizing.

The stability of the laminar boundary layer has already been studied to an appreciable extent in the literature, but most of the studies have been carried out for an impermeable wall, that is, for zero normal mass flow at the wall. A survey (as of 1952) of theoretical and experimental results related to such studies can be found in reference 2, while theoretical results of additional and later studies are summarized in reference 3. The earliest stability investigations of flow with normal mass flow at the wall were concerned with the effects of suction. References 4 to 6 show the stabilizing effect of suction in increasing the minimum critical Reynolds number of the incompressible laminar boundary layer over a flat plate with uniform suction and with a suction velocity inversely proportional to the square root of the distance from the leading edge. The laminar-boundary-layer solutions used for this purpose were the exact or numerical solutions obtained in references 7 and 8.

Investigations of the stability of flows with normal fluid injection have been made in references 9 to 11. In reference 9, the stability of the laminar boundary layer over a flat plate with a transpiration-cooled wall maintained at a uniform temperature is studied. Although the flow is here essentially at low speeds (zero or negligible Mach number), density and temperature variations in the flow are taken into account. The injection velocity at the wall is assumed to vary inversely as the square root of the distance from the leading edge, and it is shown that by a simple transformation the incompressible solutions of reference 7 can be applied. Results for the minimum critical Reynolds number show explicitly the stabilizing effect of cooling of the wall and the destabilizing effect of normal fluid injection. In reference 10, the compressible flow over a flat plate, with nonzero Mach number and uniform mass flow (both suction and injection) at the wall, is considered. The boundary-layer solutions used are, however, obtained by means of the Kármán-Pohlhausen method in

conjunction with fourth-degree velocity profiles and may, therefore, yield appreciable quantitative errors in the stability calculations (cf., e.g., ref. 12). Reference 11, which is quite recent, presents and employs exact flat-plate boundary-layer solutions which are essentially an extension to high-speed flows, that is, to nonzero Mach numbers, of the solutions used in reference 9. The use of liquid air and water as well as of air as coolants is studied. The stability calculations in reference 11 consist in determining the (uniform) wall temperature as a function of Mach number and of the injection mass-flow parameter required to stabilize completely the laminar boundary layer. These results may be considered as extensions to flow over a flat plate with normal fluid injection of the corresponding results of references 13 and 14 for an impermeable flat plate. The destabilizing effect of the normal fluid injection is illustrated here by its effect in lowering, for a given (supersonic) Mach number, the wall temperature required to stabilize the flow completely. Reference 15 contains results of stability calculations for incompressible flow in a pressure gradient with suction or injection, based on Schlichting's one-parameter integral method. The emphasis here is on the effect of a change in boundary-layer thickness on the stability of the laminar boundary layer.

In all of the foregoing research, except reference 15, on stability of laminar flows with normal mass flow at the wall, only the case of a zero pressure gradient (such as flow over a flat plate) has been considered. In the present investigation, the effect of a pressure gradient is taken into account by treating two-dimensional flows in the vicinity of a forward stagnation point over a transpiration-cooled wall. Such flows are not only of theoretical interest, but are also of practical interest, since they occur, for example, near the leading edge of a blunt-nosed object in subsonic flow. Moreover, accurate boundary-layer solutions for such flows have been derived and are tabulated in references 16 and 17. These tabulations are particularly suitable for the stability calculations to be performed here, since they include values of the first and second derivatives of the velocity and temperature profiles. The flows considered here are low-speed or zero Mach number flows, but they are nevertheless compressible in the sense that density and temperature variations are taken into account. In order to determine properly the effect of the favorable pressure gradient inherent in the stagnation flows, the stability calculations have also been performed for the flow over a flat plate, with essentially the same values of wall-temperature and injection-mass-flow parameters. The corresponding laminar-boundary-layer solutions for flow over a flat plate are also tabulated in reference 16. By calculating the minimum critical Reynolds numbers as functions of the wall-temperature and injection-mass-flow parameters for both stagnation and zero-pressure-gradient flows, the separate and simultaneous effects of wall temperature, injection mass flow, and pressure gradient are studied in the present investigation.

The stability criteria to be used in this study are primarily the approximate two-dimensional criteria developed by Lin and Lees (refs. 18 to 20) with modifications along the lines of Bloom (refs. 14, 21, and especially 22). As will be seen, however, a slight extension in these criteria is necessary for certain types of cases, including the flow over a flat plate with a normal injection mass flow at the wall. This extension is made herein. Subsequent to the completion of most of the calculations, a report by Dunn and Lin (ref. 23) appeared, in which a slightly modified set of stability criteria was developed. This report, moreover, included a treatment of three-dimensional disturbances. In the present investigation, consequently, slightly more than half of the cases were recalculated accordingly, and the results were compared with those based on the previous criteria. The comparison indicates that, although quantitative differences appear, the conclusions for the flows investigated herein based on either set of criteria remain quite similar. It will be seen, moreover, that for the low-speed though compressible flows treated herein, it is sufficient to determine the stability characteristics for only two-dimensional disturbances, since the flows will be more stable with respect to three-dimensional disturbances.

The present report is divided into three sections. In the first section the stability criteria to be used in this investigation are discussed explicitly. The mean-flow boundary-layer solutions investigated herein and the application of the stability criteria to them are then discussed in detail in the second section. Finally, the third section presents the results of the stability calculations and the conclusions drawn from them.

This research was carried out at the Polytechnic Institute of Brooklyn Aeronautical Laboratories under the sponsorship and with the financial assistance of the National Advisory Committee for Aeronautics. The authors hereby express their thanks to Professor M. Bloom for his helpful discussions.

SYMBOLS

c	dimensionless complex phase velocity of disturbance, $c_r + ic_i$ (c_r and c_i real); for a neutral disturbance, $c = c_r$
c_o	value of c at minimum critical Reynolds number
c_p	specific heat at constant pressure
f	function of η related to velocity profiles by equation (B1)

f_w value of f at wall, proportional to normal mass flow at wall (negative for injection) (cf. eqs. (29) to (32))

$G(z,\lambda)$ function in stability analysis, defined by equation (7)

$G_{min}(\lambda)$ minimum value of $G(z,\lambda)$ with respect to z for a fixed value of λ

$J(c)$ function in stability analysis, given by equation (5)

$J(z,\lambda) = 1/G(z,\lambda)$

$J_{min}(c) = 1/G_{min}(\lambda)$ (with λ as a function of c in accordance with eqs. (8) or (10))

K factor in expression for momentum thickness (eq. (35))

k coefficient of heat conductivity

L boundary-layer length (such as momentum thickness) used in stability calculations

l characteristic main-stream length (such as chord)

M Mach number

$\tilde{M}_1 = M_1(\alpha/\alpha_1)$

m exponent in equation (25)

Pr Prandtl number

R critical Reynolds number, $u_1 L/\nu_1$; that is, values of $u_1 L/\nu_1$ along neutral stability curve

$R_1 = R(\alpha/\alpha_1)$

R_b Reynolds number based on conditions at reference point outside of boundary layer, $u_b l/\nu_b$

R_{δ_i} Reynolds number based on momentum thickness, $u_1 \delta_i/\nu_1$

T absolute temperature

T_i coolant temperature

t time

u velocity in x-direction

v_w normal velocity component at wall

$w = u/u_1$

x,y coordinates parallel and normal to surface, respectively

Z coordinate perpendicular to x and y

z variable used in stability analysis (see eqs. (4) and (11))

z_o value of z corresponding to minimum value of $G(z,\lambda)$ for a fixed value of λ

α dimensionless wave number of two-dimensional disturbance (eq. (1))

$\alpha_1 = \sqrt{\alpha^2 + \beta^2}$

β proportional to dimensionless wave number in three-dimensional disturbance (eq. (22))

γ,γ_w angles defined in figure 6

δ_i momentum thickness of boundary layer

ϵ exponent in heat-conductivity—temperature relation, $k \propto T^{\epsilon}$

η variable defined by equation (26)

ϑ temperature-difference ratio, $(T - T_w)/(T_1 - T_w)$

$\vartheta_w' = \left(d\vartheta/d\eta\right)_w$

κ exponent in specific-heat—temperature relation, $c_p \propto T^{\kappa}$

λ stability profile parameter (see eqs. (8) and (10))

μ coefficient of viscosity

ν kinematic viscosity, μ/ρ

ξ dimensionless distance along wall, x/l

ρ mass density

$\Phi_r(z), \Phi_i(z)$ real and imaginary parts, respectively, of function related to Tietjens function

$\varphi(\xi)$ injection mass-flow parameter, $\left(\rho_w v_w / \rho_b u_b\right)\sqrt{R_b}$

$\bar{\varphi}$ average value of $\varphi(\xi)$ over length l

ω exponent in viscosity-temperature relation, $\mu \propto T^{\omega}$

Subscripts:

1 values at local outer edge of boundary layer

b values at reference point outside boundary layer, namely, at $x = l$

c values at $u/u_1 = c$

c_o values at $u/u_1 = c_o$

min minimum critical value, for example, R_{min}

w values at wall

A prime in the main text denotes differentiation with respect to y/L (except for ϑ_w'); in appendix A, a prime denotes differentiation with respect to y; in appendix B, it denotes differentiation with respect to η.

A bar denotes values based on equations (10) to (12) for modified two-dimensional stability criteria (except for $\bar{\varphi}$).

STABILITY CRITERIA

To aid in the physical interpretation of the results to be obtained herein, the stability criteria upon which these results are based will first be briefly reviewed and discussed. Such a brief review appears particularly worthwhile in view of the recent literature on this subject.

Curve of Neutral Disturbances

The stability criteria to be applied in the present investigation are based primarily on those developed in references 19 and 20; these

stability criteria are obtained by an extension to compressible flow of the two-dimensional theory developed in reference 18 for incompressible flow. The stability criteria are based on the amplification or decay with time of small disturbances superimposed on the steady-state boundary layer, which is assumed to be known. The disturbances Q considered are of the form

$$Q(x,y,t) = F(y)e^{i(\alpha/L)(x-cu_1t)} \tag{1}$$

(The length L and the velocity u_1 are introduced in eq. (1) so that α and c as defined there are nondimensional.) The wave number α is real and positive and is inversely proportional to the wavelength of the disturbance. The disturbance velocity c may be complex. Thus, $c = c_r + ic_i$, where $c_r u_1$ is the phase velocity of the disturbance, while c_i determines the time rate of amplification $(c_i > 0)$ or decay $(c_i < 0)$ of the disturbances. The case $c_i = 0$ defines a neutral disturbance and determines the bounds between stable and unstable flows.

By applying the Navier-Stokes equations, in conjunction with approximations pertaining to boundary-layer flows, it is found that the stability of a particular boundary layer at any given point x along the flow depends only on the local properties (such as the velocity and temperature profiles) of the boundary layer at this point and not, for example, on the previous history of the flow. This has been found to be true, as a first approximation, even when axial gradients of the disturbances and the normal velocity component of the steady-state flow are taken into account in the disturbance equations (refs. 24 to 26).[1] Thus a set of linear homogeneous partial differential equations in the disturbances is obtained, with solutions in the form of equation (1). When equation (1) is inserted into the partial differential equations, a set of linear homogeneous ordinary differential equations, with y as the independent variable, is obtained. The condition for the existence of a nontrivial solution, under appropriate homogeneous boundary conditions, then yields a relation between α and the eigenvalues c, with the Reynolds number R as a parameter. This relation can be written as two equations of the form

$$\left.\begin{aligned} c_r &= c_r(\alpha,R) \\ c_i &= c_i(\alpha,R) \end{aligned}\right\} \tag{2}$$

---

[1]It may be noted in this connection, however, that according to reference 26 the normal-velocity terms in the basic differential equations are of a larger order of magnitude than the axial-gradient terms.

By setting $c_i = 0$, which is the condition of neutral stability, a relation between α and R, of which a typical form is shown in figure 1, is obtained. For a supersonic main stream ($M_1 > 1$) at the edge of the boundary layer it is assumed that the disturbances must be subsonic, which requires, in such cases, that

$$c_r > 1 - (1/M_1) \tag{3}$$

The lower branch of the neutral curve of α versus R is asymptotic to the R-axis, that is, $R \to \infty$ as $\alpha \to 0$. The asymptotic behavior of the upper branch depends in general on the vanishing or nonvanishing of the quantity $(\partial/\partial y)(\rho\, \partial u/\partial y)$ in the local boundary layer. Thus, the upper branch also approaches the R-axis as $R \to \infty$ provided that $(\partial/\partial y)(\rho\, \partial u/\partial y) \neq 0$ in the boundary layer; otherwise, if $(\partial/\partial y)(\rho\, \partial u/\partial y) = 0$ at $u/u_1 = c_s$ say, then the upper branch has a positive asymptote, namely $\alpha \to \alpha_s$, where α_s corresponds to $c = c_s$ in the characteristic equation for an infinite value of R. The portion of the curve inside the two branches has been shown to correspond to pairs of values of α and R for which the boundary layer will be unstable, while for the pairs of values of α and R outside the loop, the flow will be stable.

Minimum Critical Reynolds Number

Of particular interest in the present investigation is the minimum value of R, called the minimum critical Reynolds number and denoted as R_{min}, on the neutral curve. From figure 1 it can be seen that R_{min} is the Reynolds number below which all (small and subsonic) disturbances, regardless of wavelength, will be damped out. Thus, a necessary condition for unstable boundary-layer flow, at least with respect to small two-dimensional disturbances of certain wavelengths, is that the actual Reynolds number at some station exceed R_{min} at that station. If the free-stream turbulence is sufficiently low, then this appears to be a necessary condition for eventual transition from a laminar to a turbulent boundary layer. Actual transition, however, occurs downstream of the point where the minimum critical Reynolds number is first exceeded and depends on additional factors such as the actual size of the disturbances and hence on their rates of amplification as well as on nonlinear effects. Even in this respect, however, the value of R_{min} may have special significance, for it is stated in references 9 and 20 that the maximum rate of amplification of the selfexcited boundary-layer disturbances varies roughly as $1/\sqrt{(R_{\delta_1})_{min}}$. Thus, the magnitude of the minimum critical Reynolds number can serve at least as a qualitative measure of the degree of stability, and hence of the tendency for transition, of a given boundary-layer flow. Since the present analysis is concerned primarily with the

effect of various parameters, such as the wall temperature and normal injection mass flow, on the stability of the laminar boundary layer, a convenient and suitable quantitative means of carrying out such an analysis is to calculate and compare the minimum critical Reynolds numbers for the various cases.

Two-Dimensional Stability Criteria and Calculation of Neutral Curve

According to the development in references 19 and 20, the neutral curve $\alpha = \alpha(R)$ involves the variable z defined as

$$z = \left(\frac{\alpha R (u/u_1)_c'}{\nu_c/\nu_1}\right)^{1/3} (y/L)_c \tag{4}$$

where the subscript c denotes values at the point where $u/u_1 = c$, called the inner critical layer. The prime here denotes differentiation with respect to y/L. The actual location of the critical layer depends largely on the function (using the notation of ref. 22)

$$J(c) = -\pi \frac{(u/u_1)_w' c (T_c/T_1)^2}{\left[(u/u_1)'\right]_c^3 (T_w/T_1)} \left[\frac{\rho}{\rho_1}\left(\frac{u}{u_1}\right)'\right]_c'$$

$$= -\pi \frac{(u/u_1)_w' c (T_c/T_1)}{\left[(u/u_1)'\right]_c^2 (T_w/T_1)} \left[\frac{(u/u_1)''}{(u/u_1)'} - \frac{(T/T_1)'}{(T/T_1)}\right]_c \tag{5}$$

(observing that $\rho/\rho_1 = T_1/T$). Along the neutral curve,

$$J(c) = J(z,\lambda) \tag{6}$$

where $J(z,\lambda)$ is a certain function of z and a boundary-layer profile parameter λ defined below by equation (8) (functions $J(z,\lambda)$ and $J(c)$ correspond, respectively, to $\psi_i(z,c)$ and $v_0(c)$ in ref. 23). The function $J(z,\lambda)$ can be expressed as (cf. refs. 22 and 23)

$$\frac{1}{J(z,\lambda)} \equiv G(z,\lambda) = \Phi_i^{-1}\left[1 - (2\Phi_r - 1)\lambda + \frac{(\Phi_r^2 + \Phi_i^2)}{(1+\lambda)}\lambda^2\right] \tag{7}$$

where $\Phi_r(z)$ and $\Phi_i(z)$ are the real and imaginary parts of a function related to the Tietjens function and can be found tabulated or plotted in references 18, 19, 20, or 23. The parameter λ is given by

$$\lambda(c) = \frac{(u/u_1)_w'}{c}\left(\frac{y}{L}\right)_c - 1 \tag{8}$$

Substituting for $(y/L)_c$ according to equation (8) into equation (4) and solving for αR yields

$$\alpha R = \frac{z^3(\nu_c/\nu_1)\left[(u/u_1)_w'\right]^3}{(u/u_1)_c' c^3(1+\lambda)^3} \tag{9}$$

An accurate determination of the wave number α according, for example, to reference 20 (eq. (27) and appendix) involves the calculation of integrals with certain types of singularities (cf. also ref. 23, where this procedure is somewhat simplified).

For any given boundary-layer flow, equations (6) and (9) and an equation for α determine points on the neutral curve in the αR plane. Thus, for a chosen value of c, $J(c)$ and $\lambda(c)$ follow from equations (5) and (8), respectively, while $J(z)$ follows from equation (7). Values of z satisfying equation (6) are then determined. If there are no values of z satisfying equation (6), then no neutral disturbance with the particular chosen (dimensionless) phase velocity c will exist for the given flow. If values of z satisfying equation (6) for a given value of c do exist, then it will be found in general that two such values occur. This is due primarily to the nature of the $G(z,\lambda)$ curves (cf. fig. 2). For each of these values of z, αR can be calculated from equation (9), while α can be determined from an additional equation. This yields a pair of values of α and R.

In a recent investigation, including three-dimensional disturbances, Dunn and Lin (ref. 23) have, for greater accuracy, slightly modified the above two-dimensional stability criteria. The parameter λ (to be denoted here by a bar) is now expressed as

$$\bar{\lambda}(c) = \frac{3}{2}\frac{(u/u_1)_w'(\nu_w/\nu_1)^{1/2}}{c^{3/2}}\int_0^{(y/L)_c}\sqrt{\frac{c-(u/u_1)}{\nu/\nu_1}}\,d\left(\frac{y}{L}\right) - 1 \tag{10}$$

Moreover, from a modified definition of z, αR (also denoted by a bar) is now given by

$$\overline{\alpha R} = z^3\left[\frac{3}{2}\int_0^{(y/L)_c}\sqrt{\frac{c-(u/u_1)}{\nu/\nu_1}}\,d\left(\frac{y}{L}\right)\right]^{-2} \tag{11}$$

With the use of equation (10), equation (11) can also be written as

$$\overline{\alpha R} = \frac{z^3(\nu_w/\nu_1)\left[(u/u_1)_w'\right]^2}{c^3(1+\lambda)^2} \tag{12}$$

Although equations (10) and (12) may in certain cases yield substantially different quantitative results from those obtained by equations (8) and (9), the new equations are on the whole essentially similar to equations (8) and (9), and in cases of very moderate temperature changes in the boundary layer the two sets of stability criteria will even yield similar quantitative results. A more detailed comparison of these two sets of criteria is given in subsequent sections.

The calculation of the neutral curve as described herein can be lengthy and tedious. If, however, it is desired only to calculate the minimum critical Reynolds number, corresponding therefore to only one point on the neutral curve (cf. fig. 1), then, with certain approximations, the calculations can be considerably simplified. Such approximations are particularly useful if, as in the present investigation, it is desired to determine the effect of various parameters, since the consistent use of an approximate set of stability criteria should suffice to give a quantitative as well as a qualitative indication of these effects.

The minimum critical Reynolds number may be assumed to correspond to that value of the wave velocity c for which there will be a single, and only a single, value of z satisfying equation (6) (refs. 22 and 23). This is equivalent to assuming that R_{min} corresponds to that value of z for which $G(z,\lambda)$ will be a minimum for a fixed value of λ (cf. fig. 2). This assumption appears reasonable since it has been seen (cf. fig. 2) that the minimum point on a $G(z,\lambda)$ curve marks the boundary below which neutral disturbances cannot exist. It may also be noted that the value of c corresponding to a minimum value of G will usually be found to be the maximum value of c for which equation (6) can be satisfied. This appears to be due primarily to the fact that $J(c)$ $(\equiv 1/G(c))$, at least in the vicinity of its intersection with the $G_{min}(c)$ or $J_{max}(c)$ curve, increases monotonically with c. These arguments are based on neglecting the variation of $\lambda(c)$ with c. This, however, appears to be justified, since, at least in the vicinity of the critical layer, it has been found that $\lambda(c)$ varies relatively very slowly with c.

In cases in which $|\lambda| \ll 1$, it follows from equation (7) that $G(z,\lambda)$ will be a minimum for a given value of c (or λ) at approximately the value of z, namely $z = 3.22$, at which $\Phi_i(z)$ is a maximum. Since at $z = 3.22$, $\Phi_i = 0.580$ and $\Phi_r = 1.50$, it follows from equation (7) that for small values of $|\lambda|$

$$G_{min}(\lambda) \approx \frac{1 - 2\lambda}{0.580} \tag{13}$$

Equation (6) then becomes

$$(1 - 2\lambda)J(c) = 0.580 \tag{14}$$

Equation (14) is the familiar approximate equation which has been developed and used in references 18 and 20 and has been applied in most approximate stability calculations.

In certain of the cases studied in the present investigation, namely, the flow over a flat plate with appreciable normal fluid injection at the wall, large negative values of λ (of the order of magnitude of -0.7) are obtained, and equation (13) (and, hence, also eq. (14)) is then no longer strictly valid. In place of equation (13), minimum values of $G(z,\lambda)$ with respect to z for various fixed values of λ can be calculated straightforwardly by means of equation (7). This has already been carried out by Bloom (ref. 22) for large positive[2] values of λ. For negative values of λ, $G(z,\lambda)$ is shown plotted in figure 3 as a function of z for various fixed values of λ when $\lambda > -1$. From figure 3, for each fixed value of λ, the values of z (to be denoted as z_o) and of G (denoted as G_{min}) at which G is a minimum are determined. The values of z_o and G_{min} as functions of λ are given in figures 4 and 5, respectively. It may be noted from figure 4 that z_o varies fairly slowly (from $z_o = 3.10$ at $\lambda = 0.1$ to $z_o = 3.74$ at $\lambda = -0.8$) with λ in the range shown; $G_{min}(\lambda)$, on the other hand, varies rapidly at appreciable negative values of λ and becomes infinitely large as $\lambda \to -1$ (fig. 5). For very low values of $|\lambda|$, it is seen from figure 5 that $G_{min}(\lambda)$ is given approximately by equation (13).

---

[2] In carrying out calculations for flow over an impermeable flat plate at high Mach numbers and large rate of cooling on the basis of equation (8), very large positive values of λ were obtained by Bloom. Using equation (10), however, Dunn and Lin (ref. 23) subsequently obtained small (positive) values of λ for all such cases of flow over an impermeable flat plate.

Physical or Geometric Significance of λ

It may be of interest to note that the stability parameter λ has a fairly simple physical or geometric significance. First, however, it should be observed that equation (10), which is the more accurate equation for λ, is, at least for cases of moderate temperature changes within the boundary layer, qualitatively quite similar to equation (8). It can, in fact, be shown (appendix A) that if ν is assumed constant, then an expansion of the velocity profiles about the critical layer $u/u_1 = c$ indicates that to a first approximation both λ and $\bar{\lambda}$ will be proportional to the second derivatives of the velocity profiles and will have the same order of magnitude. It will subsequently be seen that for all of the (low-speed) cases treated herein the values of λ and $\bar{\lambda}$ are essentially similar. (For cases of high Mach number and very large temperature changes within the boundary layer, however, eq. (10) may yield significantly different results from eq. (8) because of the presence of the kinematic viscosity ν terms in eq. (10)).

It is seen from the expansion about the critical layer (appendix A) that λ (or $\bar{\lambda}$) depends on the curvature of the velocity profiles. The geometric significance of λ can be seen particularly clearly from the approximate equation (8). From figure 6, in fact, it can be readily seen that, according to equation (8), if the velocity profile is plotted (in the customary manner) with y as ordinate and u as abscissa, then at any point on the profile

$$\lambda = \frac{\tan \gamma}{\tan \gamma_w} - 1 \tag{15}$$

where $\tan \gamma_w$ is the slope of the velocity profile $(dy/du) \equiv 1/(du/dy)$ at the wall, while $\tan \gamma$ is the slope of the secant from the origin to the given point on the velocity profile. Thus, $|\lambda|$ will be small if the velocity profile is almost linear near the wall; however, λ will, for example, have a large negative value if γ is appreciably smaller than γ_w and hence if the velocity profile has an appreciable convex curvature (cf. fig. 6). The velocity profiles for flow over a flat plate with fluid injection at the wall are found to be of the latter type. On the other hand, it will be seen that the velocity profiles for stagnation flows with or without fluid injection all have only slight curvature near the wall and hence are associated with small values of $|\lambda|$.

Calculation of c_o

The minimum critical Reynolds number depends strongly on the location of the inner critical layer, as given by the value of c. In order to determine c_o, the value of c corresponding to the minimum critical

Reynolds number, $J(c)$ and $\lambda(c)$ are first calculated as functions of c (or equivalently of $(y/L)_c$) in accordance with equations (5) and (8) or (10), respectively. For each value of c with the corresponding values of λ, $G_{min}(c)$ is obtained from figure 5. The value of c_o is the value of c for which

$$J(c) = \frac{1}{G_{min}(c)} \tag{16}$$

Equation (16) can be solved by plotting $J(c)$ and $J_{min}(c)$ and obtaining their point of intersection. Examples of such curves are given in figure 7.[3] This method of determining c_o, in conjunction with figure 5, has been consistently applied in the present report for all of the cases studied herein. (In refs. 9 to 11, where the stability of the laminar boundary layer over a flat plate with normal fluid injection is treated, no mention is made of the actual numerical values of λ obtained therein.)

Calculation of Minimum Critical Reynolds Number

In reference 9, the following approximation for the wave number α has been used for the calculation of the minimum critical Reynolds number of the laminar boundary layer over a sweat-cooled flat plate:

$$\alpha = \frac{(u/u_1)_w'}{1.2}\left(\frac{T_1}{T_w}\right)\frac{c_o}{(1 - c_o)^2}\sqrt{1 - M_1^2(1 - c_o)^2} \tag{17}$$

This expression has evidently been obtained from equation (27) of reference 20 by neglecting all terms proportional to α (or powers of α) on the right side and replacing the quantity $u - L$ by the constant 1.2. The latter approximation for $u - L$ may be adequate at least for low speeds $(M_1 \approx 0)$. The use of a simple approximate expression such as equation (17) for α introduces a considerable simplification in the stability calculations. In cases for which the wall temperature ratio T_w/T_1 does not differ greatly from unity, equation (17) is substantially similar to the more frequently used approximation developed in reference 20, namely,

$$\alpha = (u/u_1)_w' c_o\sqrt{1 - M_1^2(1 - c_o)^2} \tag{18}$$

---

[3] In the actual calculations, these curves were all plotted on more suitable individual scales. The chief purpose of figure 7 is for the subsequent comparative discussion of the results.

For $M_1 = 0$, equation (18) reduces to the approximation for α developed in reference 18 for incompressible flow.

By inserting expression (17) for α into equation (9), the following expression is obtained for the minimum critical Reynolds number:

$$R_{min} = \frac{1.2 z_o^3 \left(\nu_{c_o}/\nu_1\right)\left[\left(u/u_1\right)_w'\right]^2 \left(T_w/T_1\right)\left(1 - c_o\right)^2}{c_o^4 \left(u/u_1\right)_{c_o}' \left(1 + \lambda_{c_o}\right)^3 \left[1 - M_1^2 \left(1 - c_o\right)^2\right]^{1/2}} \tag{19}$$

Similarly, equation (12) in conjunction with equation (17) yields

$$\bar{R}_{min} = \frac{1.2 z_o^3 \left(\nu_w/\nu_1\right)\left(T_w/T_1\right)\left(u/u_1\right)_w' \left(1 - c_o\right)^2}{c_o^4 \left(1 + \bar{\lambda}_{c_o}\right)^2 \left[1 - M_1^2 \left(1 - c_o\right)^2\right]^{1/2}} \tag{20}$$

In equations (19) and (20) the subscript c_o denotes values at $u/u_1 = c_o$. Equation (20) is, in general, essentially similar to equation (19), especially in cases of small thermal changes in the boundary layer (for which $\nu_c/\nu_1 \approx \nu_w/\nu_1$) and of small curvature of the velocity profiles (for which $|\lambda|$ or $|\bar{\lambda}| \ll 1$, while $\left(u/u_1\right)_c' \approx \left(u/u_1\right)_w'$).[4] It should be noted, however, that the value of c_o to be used in equation (20) will not necessarily be exactly equal to that in equation (19), since the former should be based on expression (10) for $\bar{\lambda}$, while the latter should be based on equation (8).

It may be noted that in cases of small values of $|\lambda|$ and c_o, with T_w/T_1 close to unity, equation (19) or equation (20) reduces (except for a constant factor of $1.2 \times (3.2)^3 = 39.3$, instead of 25) to the following relatively familiar approximate expression developed in references 18 and 20:

$$R_{min} = \frac{25\left(\nu_{c_o}/\nu_1\right)\left(u/u_1\right)_w'}{c_o^4 \left[1 - M_1^2 \left(1 - c_o\right)^2\right]^{1/2}} \tag{21}$$

---

[4]Even in cases of fairly large curvature, equations (19) and (20) tend to be similar even quantitatively. For example, if $\lambda(\approx \bar{\lambda})$ is negative, then the additional $\left(1 + \lambda_{c_o}\right)$ factor in the denominator of equation (19) tends to make R_{min} greater than $\bar{R}_{min}$, but the fact that in such a case $\left(u/u_1\right)_c' > \left(u/u_1\right)_w'$ tends according to equations (19) and (20) to compensate (sometimes even overcompensate) for this effect.

In the present investigation, all of the calculations were first carried out on the basis of equation (19) in conjunction with equation (8), and subsequently, for comparison, a majority of the cases were recalculated on the basis of equation (20) in conjunction with equation (10). In all of these cases, the value of M_1 was $M_1 = 0$.

Three-Dimensional Disturbances - Extension of Squire's Theorem

The stability criteria discussed in the foregoing sections are based on two-dimensional disturbances, represented mathematically by equations of the form of equation (1). Actual disturbances may, however, be three dimensional. Such disturbances, for boundary-layer flows, can be represented in the form

$$Q(x,y,Z,t) = F(y)e^{i\left[(\alpha/L)x+(\beta/L)Z-(\alpha/L)u_1 ct\right]} \tag{22}$$

where β (as well as α) is real and positive.

For incompressible flow, it has been shown by Squire (ref. 27) that the stability equations for three-dimensional disturbances in the boundary layer can, by simple suitable transformations, be reduced to the equations of two-dimensional disturbances with wave number α_1 and Reynolds number R_1 defined by

$$\left.\begin{aligned} \alpha_1^2 &= \alpha^2 + \beta^2 \\ R_1 &= R(\alpha/\alpha_1) \end{aligned}\right\} \tag{23}$$

Since $R_1 < R$, it is concluded that any instability which may be present for a two-dimensional disturbance will also be present for a three-dimensional disturbance at a higher Reynolds number. Consequently, incompressible flows are more stable with respect to three-dimensional disturbances than with respect to two-dimensional disturbances, and it is therefore sufficient, in practice, to analyze the stability of incompressible flows with respect to only two-dimensional disturbances.

For compressible flow (at Mach numbers below the hypersonic range), it has been recently shown (refs. 23, 28, and 29) that by transformations essentially analogous to those for incompressible flow, the stability equations for three-dimensional disturbances in the boundary layer can, once again, be reduced to those for two-dimensional disturbances with wave

number α_1 and Reynolds number R_1 as given by equations (23).[5] However, the Mach number $\tilde{M}_1$ corresponding to these quasi-two-dimensional disturbances will be

$$\tilde{M}_1 = M_1(\alpha/\alpha_1) \tag{24}$$

Because of the transformation of the local Mach number as given by equation (24), the quasi-two-dimensional disturbances do not represent proper two-dimensional disturbances, and Squire's theorem on the greater stability of a given flow with respect to three-dimensional disturbances than with respect to two-dimensional disturbances is no longer strictly valid (cf. ref. 23). On the other hand, for compressible flows at zero Mach number (i.e., at low speeds), such as those to be investigated in the present report, there is no transformation of Mach number, and Squire's theorem remains valid.[6] Thus, for the cases studied herein, it is sufficient to analyze the stability with respect to only two-dimensional disturbances.

MEAN-FLOW OR STEADY-STATE SOLUTIONS

The stability criteria described in the section entitled "Stability Criteria" depend on the particular steady-state or mean-flow boundary-layer solution considered. It has been seen, moreover, that the stability criteria are fairly sensitive to first and especially to second derivatives of the velocity profiles (cf. eqs. (5)). Consequently, it is necessary that the mean-flow solutions considered be sufficiently accurate with respect to these derivatives. In the present study, such solutions are required for the case of compressible (i.e., variable density and temperature) flow with heat transfer in a pressure gradient with a small normal

---

[5]The energy equation, not considered in reference 27 for incompressible flow, appeared at first (ref. 29) to yield additional terms which do not permit a strict reduction to quasi-two-dimensional-disturbance equations. However, it is shown in reference 23 that these terms will, at least for moderate Mach numbers, be as small as other terms which have been neglected.

[6]This can be further verified from the condition (9.12) of reference 23 under which compressible three-dimensional disturbances have a minimum critical Reynolds number higher than that of two-dimensional ones. If $M_1 = 0$, then this condition will be seen to be identically satisfied. Moreover, at nonzero but subsonic free-stream Mach numbers, three-dimensional disturbances, according to reference 23, will usually have a minimum critical Reynolds number higher than that of two-dimensional ones, except possibly under conditions of extreme surface cooling.

injection velocity at the wall. Only a limited number of sufficiently accurate solutions for such fairly general cases appear to have been obtained thus far. A class of boundary-layer solutions of particular interest is that for flow over a transpiration-cooled wall with a uniform coolant, as well as a uniform wall, temperature. Approximate solutions for such flows, with arbitrarily prescribed pressure gradients and Mach numbers (below the hypersonic range), have been developed in reference 30. These, however, are based on the assumption of fourth-degree profiles and may therefore not be sufficiently accurate for stability calculations (cf. ref. 12), except, perhaps, for the stagnation flows explicitly calculated therein (cf. ref. 31). Solutions of greater accuracy for an arbitrarily prescribed pressure gradient can be developed without difficulty from the analysis in reference 1. It would merely be necessary, for this purpose, to apply sixth-degree velocity profiles (omitting the boundary condition (17d) in ref. 1) instead of the seventh-degree velocity profiles used therein. Another set of solutions for flow over a sweat-cooled wall which have been developed is that based on low-speed, but compressible, flow with the local velocity outside the boundary layer proportional to a power of the downstream distance along the wall (refs. 16, 17, and 32). Since, as will be seen, these solutions are particularly suitable for the purposes of the present investigation, these are the solutions the stability of which will be analyzed here.

Boundary-Layer Solutions for "Wedge Flows"

Flows for which the local velocity at the outer edge of the boundary layer is proportional to a power of the downstream distance along the wall have been called wedge flows since, in incompressible flow, they can represent the potential flow over wedges of various angles (see, e.g., ref. 33). Such flows can be characterized by the following nondimensional equation for the velocity distribution outside the boundary layer:

$$u_1/u_b = \xi^m \tag{25}$$

where m is a given constant, and the subscript b denotes (reference) conditions at $\xi = 1$ or $x = l$ outside the boundary layer. The pressure gradient in such a flow will be positive (adverse) or negative (favorable) according to whether $m < 0$ or $m > 0$. Such flows were originally investigated for incompressible flow over an impermeable wall in reference 34. The case $m = 0$ represents the flow over a flat plate (zero pressure gradient), while the case $m = 1$ represents the subsonic flow in the immediate vicinity of a two-dimensional forward stagnation point. These cases, therefore, have particular physical significance. For zero Mach number, as will be assumed here,

$$T_1/T_b = \rho_1/\rho_b = 1$$

along the entire flow.

In reference 32, boundary-layer solutions for flows characterized by equation (25) (especially with $m = 1$) over a sweat-cooled wall were developed for incompressible flow with constant fluid properties. Such solutions were subsequently extended in references 35, 16, and 17 to low-speed compressible flows with variable fluid properties. The wall temperature in all of these flows is assumed to be uniform. The mathematical advantage of treating such flows is that, by a fairly simple transformation, the partial differential equations of the boundary layer can be converted exactly into ordinary differential equations. Thus, a class of similar solutions is obtained, with the velocity u/u_1 and temperature T/T_1 profiles as functions of a single variable η defined by

$$\eta = y\sqrt{\frac{\rho_w u_1}{\mu_w x}} \tag{26}$$

In references 16 and 17, the boundary-layer solutions for various values of m (from $m = -0.09$ to $m = 1$) have been tabulated in detail. It has been assumed in these solutions that the viscosity, heat conductivity, and specific-heat coefficients are proportional to certain powers of the absolute temperature. Thus, it is assumed that

$$\left.\begin{aligned} \mu/\mu_w &= \left(T/T_w\right)^{\omega} \\ k/k_w &= \left(T/T_w\right)^{\epsilon} \\ c_p/c_{p_w} &= \left(T/T_w\right)^{\kappa} \end{aligned}\right\} \tag{27a}$$

The numerical values of ω, ϵ, and κ have been taken to be

$$\left.\begin{aligned} \omega &= 0.7 \\ \epsilon &= 0.85 \\ \kappa &= 0.19 \end{aligned}\right\} \tag{27b}$$

According to equations (27a) and (27b), the Prandtl number $Pr\left(\equiv \mu c_p/k\right)$ will vary very slightly according to the relation

$$Pr/Pr_w = \left(T/T_w\right)^{\omega+\kappa-\epsilon} = \left(T/T_w\right)^{0.04} \tag{27c}$$

It has been assumed in references 16 and 17 that

$$Pr_w = 0.7 \tag{27d}$$

Since the pressure is assumed to be constant across the boundary-layer thickness, the ideal gas law implies

$$\rho/\rho_1 = T_1/T \tag{28}$$

Distribution of Normal Injection Velocity

In order to obtain similar solutions of the boundary-layer partial differential equations for the cases represented by equation (25), a particular type of distribution of the normal injection mass flow along the wall must be assumed. In particular, it is assumed that f_w is constant, where f_w, which is dimensionless, is defined by

$$f_w = -\frac{2}{m+1} v_w \sqrt{\frac{\rho_w x}{\mu_w u_1}} \tag{29}$$

From equation (29), in conjunction with equations (25), (27a), and (28), it follows that the distribution of normal injection mass flow along the wall will be

$$\varphi(\xi) \equiv \frac{\rho_w v_w}{\rho_b u_b} \sqrt{\frac{\rho_b u_b l}{\mu_b}} = -f_w \left(\frac{m+1}{2}\right) \left(\frac{T_w}{T_1}\right)^{-\frac{1-\omega}{2}} \xi^{-\frac{1-m}{2}} \tag{30}$$

(f_w is negative for injection and positive for suction; l is a characteristic length in the direction of flow, not related to the boundary-layer length L in the stability equations). Thus the dimensionless injection mass-flow parameter φ will be proportional to the constant $-f_w$ and will vary inversely as the $(1 - m)/2$ power of the distance along the wall.

For stagnation flows ($m = 1$), equation (30) shows that the normal injection mass flow at the wall implicit in the similar solutions treated here will be uniform. In that case, in fact,

$$\varphi_{m=1} = -f_w \left(T_1/T_w\right)^{\frac{1-\omega}{2}} \tag{31a}$$

For flow over a flat plate ($m = 0$), on the other hand, φ will diminish along the wall from an infinitely large value at the leading edge as shown by

$$\varphi_{m=0} = -(f_w/2)(T_1/T_w)^{\frac{1-\omega}{2}} \xi^{-1/2} \tag{31b}$$

Typical distributions of $\varphi(\xi)$ are shown in figure 8.

It may be noted that for a given (negative) value of f_w and a given wall temperature ratio $T_w/T_1 (< 1)$, the average value of φ over the length l will be the same for all values of m. This follows from equation (30), according to which $\bar{\varphi}$ will be independent of m (for $m > -1$). In particular, for $m > -1$,

$$\bar{\varphi} \equiv \int_0^1 \varphi(\xi)\, d\xi = -f_w\left(\frac{T_1}{T_w}\right)^{\frac{1-\omega}{2}} \tag{32}$$

Equation (32) indicates the physical significance of the constant f_w. Thus, $-f_w$ is approximately equal to the average value along the wall of the injection mass-flow parameter φ.

Equation (30), with f_w constant, for the distribution of the normal mass-flow parameter φ has been obtained without consideration of any heat-balance equation between the fluid flowing over the wall and the cooling fluid injected through the porous wall. It can be shown, however, (cf. the section immediately following) that if such a heat balance is taken into account then the condition that the coolant temperature as well as the wall temperature be uniform yields the same type of distribution for $\varphi(\xi)$ as does equation (30).

Coolant Temperature

In references 16 and 17, a heat-balance equation at the transpiration-cooled wall was not considered. Consequently, no relation is given there between the maintained uniform wall temperature and the mass-flow constant f_w on the one hand and the coolant temperature on the other hand. Such a relation, however, can be obtained without difficulty by first expressing the condition that the heat transferred by the hot gas to the wall is absorbed by the coolant. Thus, if air is the coolant, then

$$(k\, \partial T/\partial y)_w = \rho_w v_w c_{p_w}(T_w - T_i) \tag{33}$$

where T_i is the coolant temperature, which is assumed to be uniform along the wall. Solving equation (33) for T_i and making use of equations (26) and (29) give the following expression for the coolant temperature ratio:

$$\frac{T_i}{T_l} = \frac{T_w}{T_l} - \left(\frac{2}{m+1}\right)\frac{1}{Pr_w}\frac{\vartheta_w'}{(-f_w)}\left(1 - \frac{T_w}{T_l}\right) \tag{34}$$

where $\vartheta_w' \equiv (d\vartheta/d\eta)_w$ and $\vartheta \equiv (T - T_w)/(T_l - T_w)$.

From equation (34), the (implicit) value of T_i/T_l corresponding to a pair of values of $T_w/T_l(< 1)$ and $f_w(< 0)$ can be determined for any case.[7] Corresponding values of the coolant temperature ratio are included in figure 8.

Application of Tabulated Solutions to Stability Calculations

In references 16 and 17, for a given value of m, the solutions of the ordinary differential equations for the velocity and temperature profiles are tabulated explicitly for values of η throughout the boundary-layer thickness. Moreover, first, second, and third derivatives of these solutions are also tabulated, and from them the derivatives of the velocity and temperature profiles required in the stability calculations can be easily obtained. For this reason the solutions tabulated in references 16 and 17 are especially well suited for the stability calculations to be performed in the present investigation.

In applying equations (19) and (20) to the boundary-layer profiles tabulated in references 16 and 17, the boundary-layer length L has been taken to be the momentum thickness δ_i. Application of equations (19) or (20) then yields directly the minimum critical Reynolds numbers based on the momentum thickness and the local velocity u_l. Observing that, for the boundary layers analyzed here, the momentum thickness can be expressed in the form

$$\delta_i = Kx\left(\frac{\rho_w u_l x}{\mu_w}\right)^{-1/2} \tag{35}$$

where K is independent of x (but depends on m, T_w/T_l, and f_w), the minimum critical Reynolds numbers based on the free-stream length l and the reference conditions (i.e., at point b) can be obtained. Details of the explicit equations used in the calculations are given in appendix B.

---

[7]For several of the cases treated in references 16 and 17, negative values of T_i/T_l are obtained. This simply indicates that in order to maintain the given wall temperature ratio T_w/T_l, a higher rate of mass-flow injection (i.e., a higher value of $-f_w$) would have to be used in actual practice.

STABILITY OF STAGNATION FLOWS AND FLOW OVER FLAT PLATE

In order to investigate the stability of boundary-layer flows with normal fluid injection in a pressure gradient, the minimum critical Reynolds numbers have been calculated for two-dimensional flows in the immediate vicinity of a stagnation point (eq. (25) with $m = 1$). This is a relatively simple physically significant flow with a favorable (negative) pressure gradient. In order to determine the effect of the pressure gradient, the minimum critical Reynolds numbers have also been calculated for flow in a zero pressure gradient or for flow over a flat plate (eq. (25) with $m = 0$). For both cases, the tabulated solutions in references 16 and 17, as described in the section entitled "Mean-Flow or Steady-State Solutions," have been used. For each value of m, nine different flows have been tabulated in references 16 and 17, corresponding to three different wall temperature ratios ($T_w/T_1 = 1$, $1/2$, and $1/4$) and three different values of the mass-flow injection parameter f_w ($f_w = 0$, $-1/2$, and -1). The main results of the stability calculations are given in tables I and II and in figures 7 and 9 to 13.

Effect of Cooling of Wall and of Normal Mass-Flow Injection

In figure 9, the minimum critical Reynolds numbers $\left(R_{\delta_i}\right)_{min}$ based on the momentum thickness are shown as functions of the wall temperature ratio T_w/T_1 for various fixed values of the normal injection mass-flow parameter f_w.[8] The results for both stagnation flows and flow over a flat plate are shown in this figure. For a given value of $-f_w$ it is seen that, as might be anticipated, the minimum critical Reynolds number increases, that is, the flow becomes more stable as the wall is cooled or as T_w/T_1 diminishes. This stabilizing effect of cooling of the wall (for a fixed value of $-f_w$) is seen here to be particularly pronounced for the flow over a flat plate at zero or moderate $\left(f_w = -1/2\right)$ rates of normal mass flow. It may also be observed from the nature of the curves in figure 9 that the stabilizing effect of cooling of the wall with a given value of f_w is enhanced at the lower wall temperatures.

---

[8]The square root of the minimum critical Reynolds number $\sqrt{\left(R_{\delta_i}\right)_{min}}$ is plotted here on semilogarithmic paper merely for convenience in showing all of the results on one scale. Each curve for a fixed value of f_w is based on only three calculated points. A smooth curve through these points has nevertheless been drawn in order to show clearly the trends. See also table I.

In figure 10, the minimum critical Reynolds number for both stagnation and flat-plate flows is shown as a function of the normal mass-flow parameter (cf. eq. (30))

$$\left[2/(m+1)\right]\varphi\xi^{(1-m)/2} = -f_w(T_w/T_1)^{-(1-\omega)/2}$$

for various fixed values of the wall temperature ratio T_w/T_1. Here the separate destabilizing effect of the normal mass flow can be clearly seen. This effect is seen to be especially pronounced for flow over a flat plate with a cooled wall $\left(T_w/T_1 = 1/2 \text{ and } 1/4\right)$.

The net effect of simultaneous cooling of the wall and normal fluid injection can be clearly seen from figures 9 and 10 by comparing the results with those for the case of an impermeable uncooled wall $\left(f_w = 0,\ T_w/T_1 = 1\right)$. The latter case, for the stagnation and flat-plate flows, is shown by the corresponding horizontal lines in figures 9 and 10. For each type of flow (i.e., stagnation or flat-plate flow) a net stabilizing effect of transpiration cooling is indicated by those pairs of values of f_w and T_w/T_1 or φ and T_w/T_1 on the curves in figures 9 or 10 which lie above the horizontal line corresponding to $f_w = 0$ and $T_w/T_1 = 1$. Thus, particularly from figure 10, it is seen that for the stagnation flows the net effect of transpiration cooling (with $T_w/T_1 < 1$) is stabilizing in all of the cases calculated herein, except for the case $f_w = -1$ and $T_w/T_1 = 1/2$, where the net effect is slightly destabilizing. Such is also the case for the flow over a flat plate (cf. fig. 10), except that, at the low temperature ratio $T_w/T_1 = 1/4$, the high mass-flow injection rate $\left(f_w = -1\right)$ practically cancels, or more than cancels, the separate stabilizing effect of the cooling of the wall. Flows over a highly cooled wall (e.g., $T_w/T_1 = 1/4$) with low rates of normal mass flow (e.g., $-f_w \leqq 1/2$) will, of course, be particularly stable and will have relatively high minimum critical Reynolds numbers.

From figure 11 it is seen that the results for the minimum critical Reynolds numbers based on free-stream or reference conditions are essentially similar to the above results (cf. fig. 9) based on the momentum thickness and local conditions, provided that the free-stream Reynolds numbers are plotted in the form $\left(R_b\right)_{min}\xi^{m+1}$ (see also eq. (B11)).

Effect of Pressure Gradient

The effect of the favorable pressure gradient inherent in the stagnation flows studied herein can be determined by comparing the minimum

critical Reynolds numbers for the stagnation flows with the corresponding minimum critical Reynolds numbers for flow over a flat plate. From figure 9 or figure 10 it is thus seen that in most of the cases calculated herein the stagnation flow, for the same pair of values of f_w and T_w/T_1, is more stable than the flow over a flat plate. The stabilizing effect of the favorable pressure gradient here is particularly great at the high injection rates ($f_w = -1$) regardless of the wall temperature ratio T_w/T_1, or over a relatively uncooled wall ($T_w/T_1 \approx 1$) regardless of the injection rate, for the range considered herein.

Most of the overall results thus far discussed might have been predicted qualitatively on physical grounds. Thus, the separate stabilizing effect of cooling of the wall, the separate destabilizing effect of normal mass-flow injection, and the stabilizing effect, in most of the cases, of the favorable pressure gradient appear in accord with physical expectations. A more detailed study of the results in table I and figures 9 and 10, however, reveals several interesting features which might, perhaps, have been rather difficult to anticipate intuitively.

From figure 9, it is seen that except for the case of large rates of mass-flow injection ($f_w = -1$) cooling of the wall with a fixed mass-flow parameter f_w has a considerably greater stabilizing effect on the flow over a flat plate than on stagnation flows. In fact, figure 9 indicates that, at low wall temperature ratios ($T_w/T_1 = 1/4$), $(R_{\delta_i})_{min}$ for stagnation flows will, as a result, not be higher than that for the corresponding flow over a flat plate. Thus, the stabilizing effect of the favorable pressure gradient here is greatly diminished and even eliminated at low wall temperature ratios and simultaneous zero or low ($-f_w \leq 1/2$) rates of normal mass flow. These results may, to some extent, be explained by a comparison of the velocity profiles for the various cases. Velocity profiles are shown in figures 12(a) and 12(b), together with the corresponding values of c_0 (cf. also tables II(a) and II(b)) on which the minimum critical Reynolds numbers strongly depend. Figures 12(a) and 12(b) indicate that the velocity profiles for the stagnation flows are all fairly similar near the origin (and elsewhere) and that all have concave curvature, that is, negative values of $\partial^2 u/\partial y^2$. Consequently, it may be expected that the minimum critical Reynolds numbers will all be of the same order of magnitude and will vary relatively slowly with wall temperature and normal mass flow. For flow over a flat plate, on the other hand, figures 12(a) and 12(b) reveal that the shape of the velocity profiles changes appreciably as the wall is cooled from $T_w/T_1 = 1$ to $T_w/T_1 = 1/4$ with a fixed value of f_w. This can be seen especially clearly for the case of $f_w = -1/2$. In this case, figure 12(a) shows that for an uncooled wall ($T_w/T_1 = 1$) the velocity profile near the origin has an appreciable convex curvature, that is, positive values of

$\partial^2 u/dy^2$. The latter type of curvature tends to make values of $J(c)$ algebraically small near the origin (cf. eq. (5)) and hence tends to make values of c_o large. For $f_w = -1/2$ with a highly cooled wall ($T_w/T_1 = 1/4$), however, it is seen from figure 12(b) that the velocity profile now has a concave curvature, that is, negative values of $\partial^2 u/dy^2$ with consequently algebraically higher values of $J(c)$ near the origin and a lower value of c_o. The relatively large effect of lowered wall temperature on the stability of the flat-plate flows at low rates of normal fluid injection can be further seen from figure 7. Here, for the case of zero normal mass flow, the curves $J(c)$ and $J_{min}(c)$ and their intersection (determining η_{c_o} and hence c_o) are shown for flat-plate and stagnation flows over an uncooled wall ($T_w/T_1 = 1$) and over a highly cooled wall ($T_w/T_1 = 1/4$). For the flat-plate flow, the considerable difference in the $J(c)$ curves is seen to account for the much higher value of c_o (and, hence, for the much lower value of $(R_{\delta_i})_{min}$) in the case $T_w/T_1 = 1$ than in the case $T_w/T_1 = 1/4$. For the stagnation flow, on the other hand, the $J(c)$ curves for $T_w/T_1 = 1$ and $T_w/T_1 = 1/4$ are seen to remain similar.

It has already been pointed out that at zero or low rates of mass-flow injection, the stagnation flows, despite their favorable pressure gradient, will not be more stable and may even be less stable than flow over a flat plate when the ratio of wall to free-stream static temperature is very low. This perhaps unexpected result is contrary to the trend predicted by the results of all previous stability calculations involving a pressure gradient which have invariably indicated in one manner or another the stabilizing effect of a favorable pressure gradient and the destabilizing effect of an adverse pressure gradient. The present result, however, does not contradict any of these previous results since it deals with a particular flow not included in the previous results. Thus, (assuming the correctness of the tabulated solutions in refs. 16 and 17 and of the stability criteria used herein) the present result simply shows that there exists at least one type of flow with a favorable pressure gradient, namely a two-dimensional low-speed ($M_1 \equiv 0$) stagnation flow over a highly cooled impermeable or only slightly porous wall, which has a lower minimum critical Reynolds number based on momentum thickness than the corresponding flow without a pressure gradient. A partial explanation of this result can be given by comparing velocity profiles and noting from figure 12(b), for the case of $T_w/T_1 = 1/4$, that near the origin the velocity profiles for the flat-plate flow behave similarly to those for the stagnation flow when $f_w = 0$ or $-1/2$ (in contrast, e.g., with the considerable change of the flat-plate profile when $f_w = -1$, or with the different appearance of the flat-plate velocity profiles from that of the stagnation profiles when the wall is uncooled (cf. figs. 12(a) and 7).

From a practical viewpoint, the fact that the stability limit of the stagnation flow is apparently lower than that of the flat-plate flow at low or zero rates of injection over a highly cooled wall does not appear very serious. First of all, the difference in the values of $(R_{\delta_i})_{min}$ is not very great.[9] Moreover, the minimum critical Reynolds numbers in both cases are so high that both types of flow may, for practical purposes, be regarded as completely stable. The present result nevertheless appears to be of considerable theoretical interest while it may also be of practical interest if other cases of an apparent destabilizing nature of a favorable pressure gradient exist. It would therefore appear worthwhile to investigate this problem further. For example, a recalculation of the present results based on mean-flow solutions obtained independently of those in references 16 and 17 may be worthwhile. Moreover, the extension of the present results for stagnation and flat-plate flows to still more highly cooled walls ($T_w/T_1 < 1/4$) would be of interest to determine whether the trends indicated in figure 9 continue as T_w/T_1 is decreased beyond 1/4. Finally, an analysis of the stability of low-speed flows with pressure gradients other than stagnation flows, such as flows characterized by $u_1/u_b = 1 \pm a\xi$ (where a is a positive constant), over a highly cooled wall might reveal whether the result obtained herein is peculiar only to special types of flows such as stagnation flows. A calculation of the stability of three-dimensional stagnation flows (corresponding to $m = 1/3$) would also be of interest.

From figure 10 (cf. also table I), it is seen that, except for the case of the uncooled wall, normal fluid injection with a fixed wall temperature ratio T_w/T_1 has an appreciably greater destabilizing effect on flow over a flat plate than on a stagnation flow. This effect is especially pronounced for the highly cooled wall ($T_w/T_1 = 1/4$) at the high rate of fluid injection $(f_w = -1)$. Once again this can be largely explained by referring to the velocity profiles in figure 12(b) ($T_w/T_1 = 1/4$) where, for example, the considerable change in the flat-plate velocity profile as f_w changes from -1/2 to -1 can be clearly seen. The stagnation profiles, on the other hand, tend to remain similar as f_w varies from 0 to -1, regardless of the wall temperature (cf. figs. 12(a) and 12(b)). It is interesting, however, to note that, for

---

[9] In this connection, it may also be noted that the minimum critical Reynolds number based on main-stream reference conditions $(R_b)_{min}$ will vary inversely as ξ^2 for stagnation flows but inversely as ξ for flat-plate flows (cf. eq. (B11)). Consequently, for the same value of $(R_{\delta_i})_{min}/K$, $(R_b)_{min}$ for stagnation flows would exceed that for flat-plate flows at $\xi < 1$. In fact, according to table I, for the interesting case $T_w/T_1 = 1/4$ and $f_w = 0$, $(R_b)_{min}$ for the stagnation flows will exceed that for flow over a flat plate at $\xi < 13{,}510/24{,}900$ or 0.543.

an uncooled or only moderately cooled wall, the stability of the flat-plate flows, in contrast with that of the stagnation flows, tends to become relatively less and less sensitive to changes in the normal mass-flow injection when the rate of the latter is high (cf. fig. 10). (This appears, in part, to be due mathematically to the large negative values of λ for flat-plate flows with high injection rates, which tend to prevent $(R_{\delta_i})_{min}$ from diminishing sharply (eqs. (19) or (20)).

Effect of Coolant Temperature

For a fixed rate of mass-flow injection $\varphi(\xi)$, which corresponds approximately to a fixed value of f_w (for a given value of m and a fixed value of $\varphi(\xi)$, f_w depends slightly on the wall temperature ratio T_w/T_1 (eqs. (30) to (31b)), lowering the coolant temperature T_i will lower the wall temperature T_w. This, as has just been seen, will stabilize the boundary layer by increasing the minimum critical Reynolds number. An example of this effect is shown in figure 13, where, for a fixed value of $f_w(= -1)$, the minimum critical Reynolds number is given as a function of the coolant temperature ratio T_i/T_1 for both flat-plate and stagnation flows.

It might also be of interest to calculate the stability of the boundary layer for a fixed coolant temperature ratio T_i/T_1 and a varying rate of mass-flow injection. This has been carried out in reference 9 for (low-speed) flow over a flat plate. It has been shown there that for a fixed value of T_i/T_1 there will be a value of the injection rate (essentially f_w) for which the minimum critical Reynolds number will be a maximum. A similar calculation would be of interest for stagnation flows. However, boundary-layer solutions in addition to those tabulated in references 16 and 17 would be required for this purpose. One possibility might be to apply consistently the approximate solutions in reference 30.

Comparison of Stability Criteria

The stability of all of the flows studied herein has been calculated by means of equations (8) and (19). In view, however, of the quite recent appearance of reference 23, a majority of the cases have been recalculated, for comparison, on the basis of equations (10) and (20), which are given in reference 23 as a modification, for greater accuracy, of equations (8) and (19). It has already been seen that these two sets of equations are, on the whole, essentially similar, especially for low-speed flows and moderate temperature changes within the boundary layer (cf. the section entitled "Stability Criteria"). The results of the calculations based on

equations (10) and (20) are shown in tables II(a) and II(b) and in figure 10. Figure 10 indicates that, although some quantitative differences occur, the conclusions based on the results of equations (8) and (19) remain on the whole unchanged. It is, furthermore, significant to note, from tables II(a) and II(b), that the values of λ calculated according to equation (10) are essentially similar to those based on equation (8) and that the calculated values of c_o consequently remain on the whole quite similar. (When $|\lambda| \ll 1$, then the actual numerical value of λ, whether it is positive or negative, will not have a great influence on the stability calculations.)

It is noteworthy that for the stagnation flows studied here the absolute values of the profile stability parameter λ are all much smaller than unity (cf. table II(b)) regardless of the wall temperature ratio or of the mass-flow injection parameter f_w. For the flow over a flat plate, however, relatively high negative values of λ occur when the rate of mass-flow injection is high (cf. table II(a)). This is readily explained by a glance at the various velocity profiles in figures 12(a) and 12(b) and a comparison of them with figure 6 (cf. also the section entitled "Stability Criteria"). The velocity profiles for the flat-plate flows at $f_w = -1$ are thereby readily seen to be associated with high negative values of λ.

CONCLUSIONS

The minimum critical Reynolds number as a function of the wall temperature and the normal mass-flow injection has been calculated for the laminar boundary layer over a transpiration-cooled wall maintained at a uniform temperature in the low-speed, but compressible, flow over a flat plate and in the immediate vicinity of a two-dimensional forward stagnation point. From these results, the following main conclusions have been drawn:

(1) For a given rate of mass-flow injection, cooling of the wall stabilizes the flow by increasing the minimum critical Reynolds number. This effect is enhanced at the lower wall temperatures. At a fixed wall temperature, an increase of normal mass-flow injection destabilizes the laminar boundary layer by decreasing the minimum critical Reynolds number. The net effect of simultaneous cooling of the wall and normal fluid injection can be readily seen from the results obtained herein by comparing the minimum critical Reynolds numbers for this flow with those for flow over an uncooled impermeable wall. In most, though not all, of the particular cases calculated herein, the net effect was found to be stabilizing.

(2) In most of the cases, the favorable pressure gradient inherent in the stagnation flows has an appreciable stabilizing effect on the

laminar boundary layer. This effect is especially pronounced at the high injection rates regardless of the wall temperature and over an uncooled or only slightly cooled wall regardless of the injection rate.

(3) Except for the case of large rates of mass-flow injection, cooling of the wall, with a fixed rate of normal mass-flow injection, has a considerably greater stabilizing effect on the flow over a flat plate than on stagnation flows. At low ratios of wall temperature to free-stream temperature, in fact, the minimum critical Reynolds numbers for stagnation flows will consequently not be higher than that for the corresponding flow over a flat plate. Thus, the stabilizing effect of the favorable pressure gradient in stagnation flows is greatly diminished, and even eliminated or reversed, at low ratios of wall to free-stream temperature and simultaneous zero or low rates of mass-flow injection. In view of this somewhat unexpected result, it would be of interest to investigate the stability of stagnation flows over still more highly cooled walls and to investigate the stability of other types of flows with pressure gradients at low local speeds over a highly cooled wall.

(4) Except for the case of an uncooled or very slightly cooled wall, normal fluid injection with a fixed wall temperature has a considerably greater destabilizing effect on flow over a flat plate than on a stagnation flow. This effect was found to be especially pronounced for the highly cooled wall at the high rates of fluid injection calculated herein.

(5) For a fixed rate of mass-flow injection, lowering the coolant temperature will lower the wall temperature and hence will stabilize the boundary layer by increasing the minimum critical Reynolds number.

(6) The velocity profiles for flow over a flat plate with high rates of mass-flow injection at the wall are of the type which lead to relatively large negative values of a stability parameter λ. The approximate stability criteria have been slightly modified herein for such cases.

Polytechnic Institute of Brooklyn,
Brooklyn, N. Y., November 16, 1955.

APPENDIX A

COMPARISON OF EQUATIONS (8) AND (10) FOR BOUNDARY-LAYER PROFILE PARAMETER $\lambda(c)$

A qualitative comparison of equations (8) and (10) for $\lambda(c)$ can be made by expanding the velocity profile $w \equiv u/u_1$ about the critical layer $w = c$ (or $y = y_c$). Thus, let

$$w = c + w_c'(y - y_c) + \frac{w_c''}{2!}(y - y_c)^2 + \cdots \tag{A1}$$

where a prime indicates $\partial/\partial y$. To satisfy the condition $u = 0$ at $y = 0$, it is necessary, according to equation (A1), that

$$c - w_c' y_c + \frac{w_c''}{2!} y_c^2 - \cdots = 0 \tag{A2}$$

Moreover, according to equation (A1),

$$\int_0^{y_c} \sqrt{c - (u/u_1)}\, dy = \int_0^{y_c} \sqrt{w_c'\zeta - \frac{w_c''}{2!}\zeta^2 + \cdots}\, d\zeta \tag{A3}$$

where $\zeta = y_c - y$. Applying the binomial expansion in equation (A3) yields

$$\int_0^{y_c} \sqrt{c - (u/u_1)}\, dy = \frac{2}{3}(w_c')^{1/2} y_c^{3/2} - \frac{1}{10}(w_c')^{-1/2} w_c'' y_c^{5/2} + \cdots \tag{A4}$$

From equation (A1),

$$w_w' = w_c' - w_c'' y_c + \cdots \tag{A5}$$

Hence, when $\nu/\nu_1 \approx 1$ in the region $0 \leqq y \leqq y_c$, equation (10) yields

$$\bar{\lambda}(c) = \frac{3}{2}\frac{(w_c' - w_c''y_c + \cdots)}{c^{3/2}}\left[\frac{2}{3}(w_c')^{1/2}y_c^{3/2} - \frac{1}{10}(w_c')^{-1/2}w_c''y_c^{5/2} + \cdots\right] - 1$$

$$= \left(\frac{w_c'}{c}y_c\right)^{3/2} - \frac{23}{20}\left(\frac{w_c'}{c}y_c\right)^{1/2}\frac{y_c^2}{c}w_c'' + \cdots - 1 \qquad (A6)$$

From equation (A2),

$$\frac{w_c'}{c}y_c = 1 + \frac{w_c''y_c^2}{2c} - \cdots \qquad (A7)$$

Substitution for $(w_c'y_c/c)$ into equation (A6) yields, to the second power of y_c,

$$\bar{\lambda}(c) = -\frac{2}{5}\frac{w_c''}{c}y_c^2 + \cdots \qquad (A8)$$

With the use of equations (A5) and (A7), equation (8) yields the following expression for $\lambda(c)$, to the second power of y_c:

$$\lambda(c) = -\frac{1}{2}\frac{w_c''}{c}y_c^2 + \cdots \qquad (A9)$$

Equations (A8) and (A9) show that, to second powers of y (and y_c), equations (8) and (10) with ν constant yield the same results for $\lambda(c)$ except for a slight difference in the numerical factors. Thus, it is seen that λ and $\bar{\lambda}$ depend on substantially similar properties of the velocity profiles and will both be of the same order of magnitude.

If temperature changes within the boundary layer are taken into account and it is assumed that

$$\nu/\nu_1 = \nu_c/\nu_1 + (\nu/\nu_1)_c'(y - y_c) + \cdots \qquad (A10)$$

then equation (A9) remains unchanged, while equation (A8) becomes

$$\bar{\lambda}(c) = -\frac{y_c^2}{5c}\left(2w_c'' + \cdots + w_c'\frac{\nu_c'}{\nu_c} + \cdots\right) \qquad (A11)$$

If $\nu' > 0$, as will be the case for low-speed flows with $T_w/T_1 < 1$, then the ν terms in equation (10) will tend to make $\bar{\lambda}$ algebraically less than λ. This will tend to increase $G_{min}(\lambda)$ (cf. fig. 5) or to decrease J_{min} and hence to decrease c_o.

In cases for which $|\lambda| \ll 1$ (e.g., $|\lambda| \leq 0.02$), it will be found that the stability criteria tend to be relatively insensitive to the actual numerical value of λ.

APPENDIX B

CALCULATION OF MINIMUM CRITICAL REYNOLDS NUMBER

In the solutions of references 16 and 17, the functions f, f', f'', f''', ϑ, ϑ', and ϑ'' are tabulated, for any given case, as functions of η, where η is defined by equation (26) in conjunction with equation (25). Primes denote here derivatives with respect to η. The functions f and ϑ are related to the velocity and temperature profiles in accordance with the relations

$$\frac{u}{u_1}(\eta) = f'(\eta)\left[1 + \left(\frac{T_1}{T_w} - 1\right)\vartheta\right] \tag{B1}$$

$$\frac{T}{T_1}(\eta) = \frac{T_w}{T_1} + \left(1 - \frac{T_w}{T_1}\right)\vartheta(\eta) \tag{B2}$$

From equations (B1) and (B2) it follows that the derivatives of the velocity and temperature profiles can be calculated by means of the relations

$$\left.\begin{aligned}
\left(\frac{u}{u_1}\right)' &= f'' + \left(\frac{T_1}{T_w} - 1\right)(f''\vartheta + f'\vartheta') \\
\left(\frac{u}{u_1}\right)'' &= f''' + \left(\frac{T_1}{T_w} - 1\right)(f'''\vartheta + 2f''\vartheta' + f'\vartheta'') \\
\left(\frac{T}{T_1}\right)' &= \left(1 - \frac{T_w}{T_1}\right)\vartheta'
\end{aligned}\right\} \tag{B3}$$

Since the expression for $J(c)$, as given by equation (5), is independent of the boundary-layer length L, the differentiations indicated in equation (5) have been carried out with respect to η. Similarly, in expressions (8) and (10) for λ and $\bar{\lambda}$, which are also independent of L, y/L has been chosen to be η. Thus,

$$\lambda(c) = \left(u/u_1\right)_w' \frac{\eta_c}{c} - 1 \tag{B4}$$

Moreover, since in accordance with equations (27a) and (28),

$$\nu/\nu_1 = (T/T_1)^{1+\omega} \tag{B5}$$

equation (10) becomes

$$\bar{\lambda}(c) = \frac{3}{2}\frac{(u/u_1)_w'}{c^{3/2}}\left(\frac{T_w}{T_1}\right)^{\frac{1+\omega}{2}}\int_0^{\eta_c}\sqrt{\frac{c - (u/u_1)}{(T/T_1)^{1+\omega}}}\,d\eta - 1 \tag{B6}$$

where $\omega = 0.7$.

The expressions on either side of equations (19) and (20) do depend on the boundary-layer length L. For the present calculations, the length L has been chosen in these equations as the momentum thickness δ_i. From equations (26) and (35) it follows that

$$\eta = K(y/\delta_i) \tag{B7}$$

Thus, equations (19) and (20), in conjunction with equation (B5), yield, respectively, the following expressions for the minimum critical Reynolds number based on the momentum thickness:

$$(R_{\delta_i})_{min} \equiv \left(\frac{u_1\delta_i}{\nu_1}\right)_{min} = \frac{1.2Kz_o^3(T/T_1)_{c_o}^{(1+\omega)}\left[(u/u_1)_w\right]^2(T_w/T_1)(1 - c_o)^2}{c_o^4(u/u_1)_{c_o}'\left(1 + \bar{\lambda}_{c_o}\right)^3\left[1 - M_1^2(1 - c_o)^2\right]^{1/2}} \tag{B8}$$

$$\left(\overline{R_{\delta_i}}\right)_{min} \equiv \left(\overline{\frac{u_1\delta_i}{\nu_1}}\right)_{min} = \frac{1.2Kz_o^3\left(T_w/T_1\right)^{(2+\omega)}\left(u/u_1\right)_w'(1 - c_o)^2}{c_o^4\left(1 + \bar{\lambda}_{c_o}\right)^2\left[1 - M_1^2(1 - c_o)^2\right]^{1/2}} \tag{B9}$$

In the present calculations $M_1 = 0$.

The minimum critical Reynolds numbers based on reference conditions (at point b) and the main-stream characteristic length l can be obtained from the results of equations (B8) and (B9) by using expression (35) for δ_i. Thus, from equation (35) it follows that

$$\frac{u_1 x}{\nu_1} = \left(\frac{R_{\delta_i}}{K}\right)^2\left(\frac{\nu_1}{\nu_w}\right) \tag{B10}$$

With $\xi \equiv x/l$, $\nu_1 = \nu_b$, and $u_1 = u_b\xi^m$, equation (B10) in conjunction with equation (B5) yields

$$\left(R_b\right)_{min}\xi^{m+1} \equiv \left(\frac{u_b l}{\nu_b}\right)_{min}\xi^{m+1} = \left(\frac{R\delta_1}{K}\right)_{min}^2\left(\frac{T_1}{T_w}\right)^{1+\omega} \tag{B11}$$

From equations (B8) or (B9) and (B11) it follows that $\left(R_b\right)_{min}$ is independent of the momentum-thickness factor K.

REFERENCES

1. Morduchow, Morris: Laminar Separation Over a Transpiration-Cooled Surface in Compressible Flow. NACA TN 3559, 1955.

2. Gazley, Carl, Jr.: Boundary-Layer Stability and Transition in Subsonic and Supersonic Flow. Jour. Aero. Sci., vol. 20, no. 1, Jan. 1953, pp. 19-28.

3. Morduchow, Morris: Analysis and Calculation by Integral Methods of Laminar Compressible Boundary Layer With Heat Transfer and With and Without Pressure Gradient. NACA Rep. 1245, 1955.

4. Ulrich, A.: Die Stabilität der laminaren Reibungsschicht an der ebenen Platte mit Absaugen und Ausblasen. U. M. 2044, Deutsche Luftfahrtforschung, June 11, 1943.

5. Ulrich, A.: Die Stabilität der laminaren Reibungsschicht an der ebenen Platte mit homogener Absaugung. U. M. 2033, Deutsche Luftfahrtforschung, Nov. 1, 1943.

6. Hahneman, Elizabeth, Freeman, J. C., and Finston, M.: Stability of Boundary Layers and of Flow in Entrance Section of a Channel. Jour. Aero. Sci., vol. 15, no. 8, Aug. 1948, pp. 493-496.

7. Schlichting, H., and Bussman, K.: Exakte Lösungen für die laminare Grenzschicht mit Absaugung und Ausblasen. Schr., Deutsche Akad. Luftfahrtforschung, Bd. 7B, Heft 2, 1943, pp. 25-69.

8. Iglisch, R.: Exakte Berechnung der laminaren Grenzschicht an der Längangeströmten ebenen Platte mit homogener Absaugung. Schr., Deutsche Akad. Luftfahrtforschung, Bd. 8B, Heft 1, 1944. (Available in English translation as NACA TM 1205.)

9. Lees, Lester: Stability of the Laminar Boundary Layer With Injection of Cool Gas at the Wall. Aero. Eng. Lab. Rep. 139, Princeton Univ., May 20, 1948.

10. Libby, Paul A., Lew, Henry G., and Romano, Frank J.: On the Stability of a Laminar Compressible Boundary Layer Over a Flat Plate Subject to Uniform Suction and Injection. PIBAL Rep. 133, Polytechic Inst. of Brooklyn, Oct. 15, 1948.

11. Low, George M.: The Compressible Laminar Boundary Layer With Fluid Injection. NACA TN 3404, 1955.

12. Libby, Paul A., Morduchow, Morris, and Bloom, Martin: Critical Study of Integral Methods in Compressible Laminar Boundary Layers. NACA TN 2655, 1952.

13. Van Driest, E. R.: Calculation of the Stability of the Laminar Boundary Layer in a Compressible Fluid on a Flat Plate With Heat Transfer. Jour. Aero. Sci., vol. 19, no. 12, Dec. 1952, pp. 801-812, 828.

14. Bloom, Martin: The Effect of Surface Cooling on Laminar Boundary-Layer Stability. Readers' Forum, Jour. Aero. Sci., vol. 18, no. 9, Sept. 1951, pp. 635-636.

15. Tetervin, Neal, and Levine, David A.: A Study of the Stability of the Laminar Boundary Layer as Affected by Changes in the Boundary-Layer Thickness in Regions of Pressure Gradient and Flow Through the Surface. NACA TN 2752, 1952.

16. Brown, W. Byron, and Donoughe, Patrick L.: Tables of Exact Laminar-Boundary-Layer Solutions When the Wall Is Porous and Fluid Properties Are Variable. NACA TN 2479, 1951.

17. Brown, W. Byron, and Livingood, John N. B.: Solutions of Laminar-Boundary-Layer Equations Which Result in Specific-Weight-Flow Profiles Locally Exceeding Free-Stream Values. NACA TN 2800, 1952.

18. Lin, C. C.: On the Stability of Two-Dimensional Parallel Flows. Part I, Quart. Appl. Math., vol. III, no. 2, July 1945, pp. 117-142; Part II, vol. III, no. 3, Oct. 1945, pp. 218-234; and Part III, vol. III, no. 4, Jan. 1946, pp. 277-301.

19. Lees, Lester, and Lin, Chia Chao: Investigation of the Stability of the Laminar Boundary Layer in a Compressible Fluid. NACA TN 1115, 1946.

20. Lees, Lester: The Stability of the Laminar Boundary Layer in a Compressible Fluid. NACA Rep. 876, 1947. (Supersedes NACA TN 1360.)

21. Bloom, Martin: Further Comments on "The Effect of Surface Cooling on Laminar Boundary-Layer Stability." Readers' Forum, Jour. Aero. Sci., vol. 19, no. 5, May 1952, p. 359.

22. Bloom, Martin: On the Calculation of Laminar Boundary-Layer Stability. Readers' Forum, Jour. Aero. Sci., vol. 21, no. 3, Mar. 1954, pp. 207-210.

23. Dunn, D. W., and Lin, C. C.: On the Stability of the Laminar Boundary Layer in a Compressible Fluid. Jour. Aero. Sci., vol. 22, no. 7, July 1955, pp. 455-477.

24. Pretsch, J.: Die Stabilität der Laminarströmung bei Druckgefälle und Druckanstieg. Forschungsbericht Nr. 1343, Deutsche Luftfahrtforschung, 1941.

25. Laurmann, J. A.: Stability of the Compressible Laminar Boundary Layer With an External Pressure Gradient. Rep. 48, College of Aero. (Cranfield), Sept. 1951.

26. Cheng, Sin-I: On the Stability of Laminar Boundary Layer Flow. Quart. App. Math., vol. XI, no. 3, Oct. 1953, pp. 346-350.

27. Squire, H. B.: On the Stability for Three-Dimensional Disturbances of Viscous Fluid Flow Between Parallel Walls. Proc. Royal Soc. of London, ser. A., vol. 142, no. 847, Nov. 1933, pp. 621-628.

28. Dunn, D. W., and Lin, C. C.: The Stability of the Laminar Boundary Layer in a Compressible Fluid for the Case of Three-Dimensional Disturbances. Readers' Forum, Jour. Aero. Sci., vol. 19, no. 7, July 1952, p. 491.

29. Lessen, Martin: On the Stability of Plane Parallel Laminar Flows to Two- and Three-Dimensional Disturbances. Readers' Forum, Jour. Aero. Sci., vol. 19, no. 6, June 1952, pp. 431-432.

30. Morduchow, Morris: On Heat Transfer Over a Sweat-Cooled Surface in Laminar Compressible Flow With a Pressure Gradient. Jour. Aero. Sci., vol. 19, no. 10, Oct. 1952, pp. 705-712.

31. Morduchow, Morris, and Clarke, Joseph H.: Method for Calculation of Compressible Laminar Boundary-Layer Characteristics in Axial Pressure Gradient With Zero Heat Transfer. NACA TN 2784, 1952.

32. Eckert, E. R. G.: Heat Transfer and Temperature Profiles in Laminar Boundary Layers on a Sweat-Cooled Wall. A.A.F. Tech. Rep. 5646, Air Material Command, Nov. 1947.

33. Prandtl, L., and Tietjens, O. G. (L. Rosehead, trans.): Fundamentals of Hydro- and Aeromechanics. McGraw-Hill Book Co., Inc., 1934, pp. 162-166.

34. Falkner, V. M., and Skan, Sylvia W.: Some Approximate Solutions of the Boundary Layer Equations. R. & M. No. 1314, British A.R.C., 1930.

35. Brown, W. Byron: Exact Solutions of the Laminar Boundary Layer Equations for a Porous Plate With Variable Fluid Properties and a Pressure Gradient in the Main Stream. Presented at First U. S. Nat. Cong. of Appl. Mech. (Chicago), June 11-16, 1951, pp. 843-852.

TABLE I.- MINIMUM CRITICAL REYNOLDS NUMBERS AS FUNCTIONS OF WALL TEMPERATURE AND RATE OF NORMAL MASS-FLOW INJECTION

$\frac{T_w}{T_1}$	f_w	Stagnation flow, $u_1/u_b = \xi$		Flow over flat plate, $u_1/u_b = 1$	
		$(R_{\delta_1})_{min}$	$(R_b)_{min}\,\xi^2$	$(R_{\delta_1})_{min}$	$(R_b)_{min}\,\xi$
1	0	4.20×10^3	21.0×10^7	0.104×10^3	0.00248×10^7
	-1/2	2.43	4.97	.0225	.0000750
	-1	1.36	1.13	.0151	.0000197
$\frac{1}{2}$	0	22.4	339	12.5	31.2
	-1/2	8.62	31.3	.244	.00754
	-1	2.49	1.53	.0414	.000124
$\frac{1}{4}$	0	159	13,510	378	24,900
	-1/2	58.0	1,023	85.0	793
	-1	5.37	4.55	.100	.000615

TABLE II.- DETAILS OF STABILITY CALCULATIONS

(a) Flow over a flat plate

$\frac{T_w}{T_1}$	f_w	Based on eqs. (8) and (19)			Based on eqs. (10) and (20)		
		λ_{c_o}	c_o	$(R_{\delta_1})_{min}$	$\bar{\lambda}_{c_o}$	c_o	$(\bar{R}_{\delta_1})_{min}$
1	0	0.015	0.415	[a]0.104×10^3	0.011	0.413	0.100×10^3
	-1/2	-.226	.548	.0225	-.196	.547	.0232
	-1	-.703	.620	.0151	-.663	.622	.0192
$\frac{1}{2}$	0	0.035	0.114	12.5			
	-1/2	-.098	.279	.244			
	-1	-.702	.459	.0414			
$\frac{1}{4}$	0	0.039	[b]0.0367	378	-0.009	0.034	486
	-1/2	-.012	[b].0473	85.0	-.050	.044	108
	-1	-.735	.319	.100	-.76	.312	.0665

(b) Flow near a forward stagnation point

$\frac{T_w}{T_1}$	f_w	Based on eqs. (8) and (19)			Based on eqs. (10) and (20)		
		λ_{c_o}	c_o	$(R_{\delta_1})_{min}$	$\bar{\lambda}_{c_o}$	c_o	$(\bar{R}_{\delta_1})_{min}$
1	0	0.082	0.210	4.20×10^3	0.068	0.207	3.99×10^3
	-1/2	.080	.229	2.43	.055	.223	2.74
	-1	.068	.258	1.36	.058	.255	1.36
$\frac{1}{2}$	0	0.033	0.110	22.4			
	-1/2	.055	.132	8.62			
	-1	.046	.171	2.49			
$\frac{1}{4}$	0	0.049	[b]0.0490	159	-0.003	0.044	238
	-1/2	.038	[b].0601	58.0	-.005	.059	59.0
	-1	.023	.102	5.37	-.014	.096	6.52

[a]The accurate value of $(R_{\delta_1})_{min}$ for this case, based on an exact calculation of neutral stability curve, without approximate criteria used herein, is 150 to 162 (refs. 20 and 18, respectively). Values based on particular simplified approximate criteria as given by eq. (21) range from 180 to 195 (refs. 12 and 20, respectively), which are too high. Value obtained herein is evidently too low. These differences from exact value, however, are usually not regarded as very significant in stability calculations. It is important to note that in all of these calculations (i.e., refs. 12, 18, 20, and present report) for this case, value of c_o is practically same.

[b]Because of closeness of c_o to zero in these cases, determination of c_o was based on expanding velocity and temperature profiles in a Taylor series about origin, using tabulated values of derivatives at origin and obtaining values of additional higher derivatives from governing ordinary differential equations.

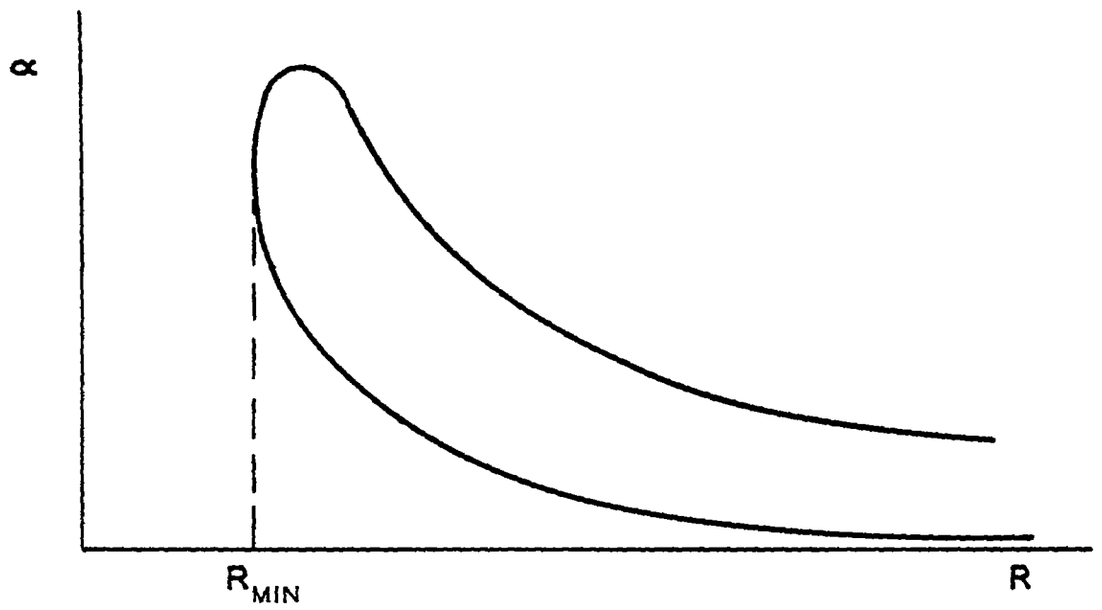

Figure 1.- Typical curve of neutral stability.

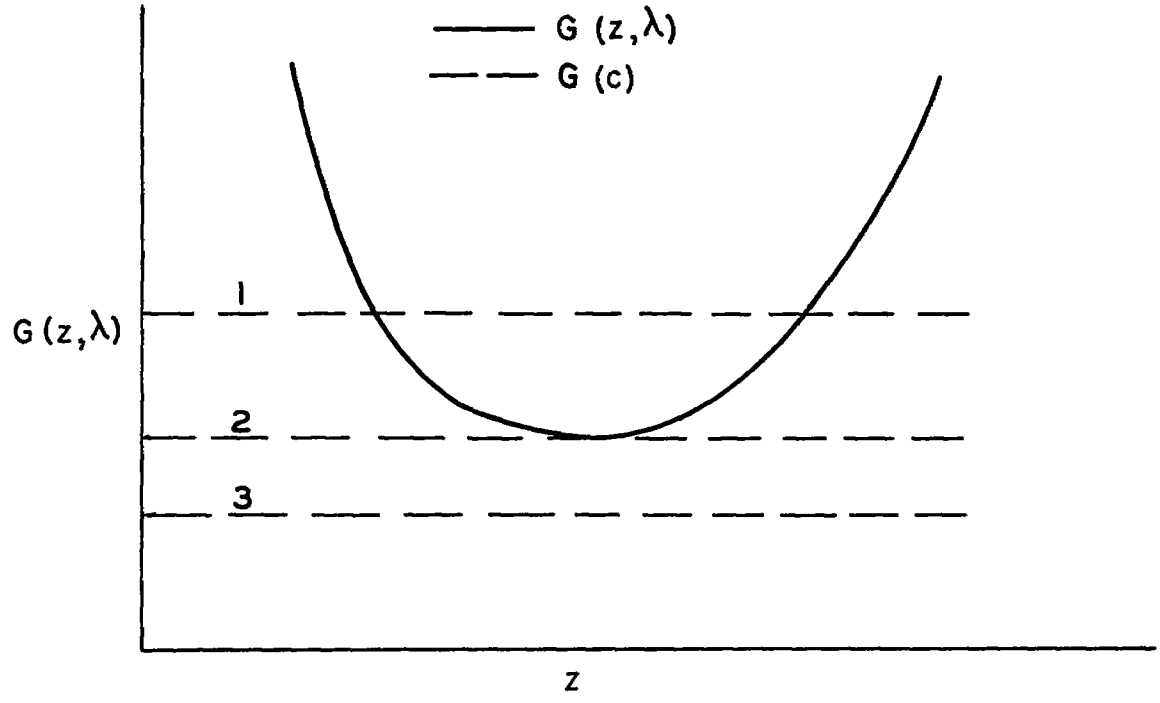

Figure 2.- Typical curve of $G(z,\lambda)$ versus z for a fixed value of λ. Numbers indicate: 1, two values of z for chosen value of c satisfying equation (6); 2, one value of z for chosen value of c satisfying equation (6); and 3, no values of z for chosen value of c satisfying equation (6).

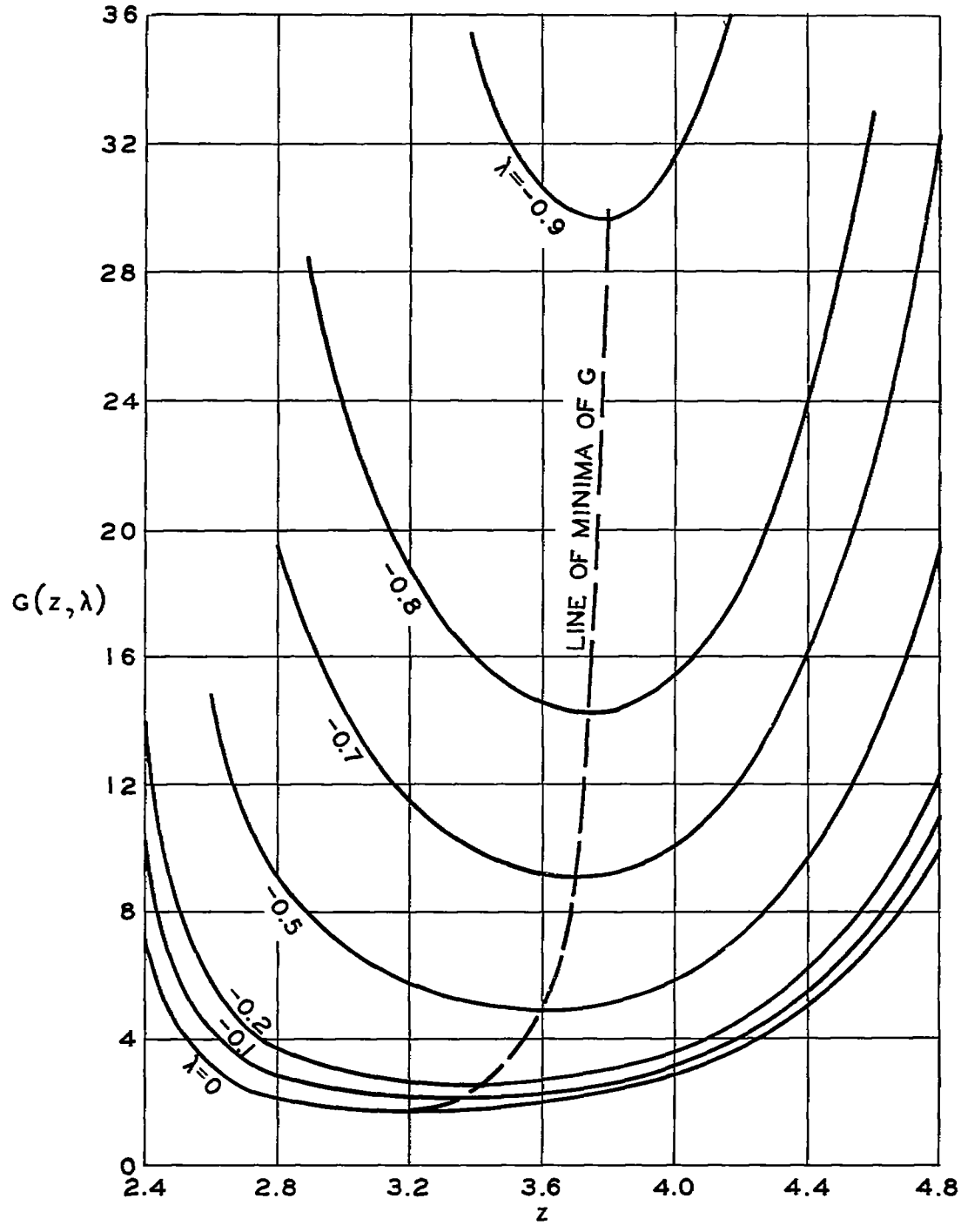

Figure 3.- Plot of $G(z,\lambda)$ as function of z for various fixed negative values of λ.

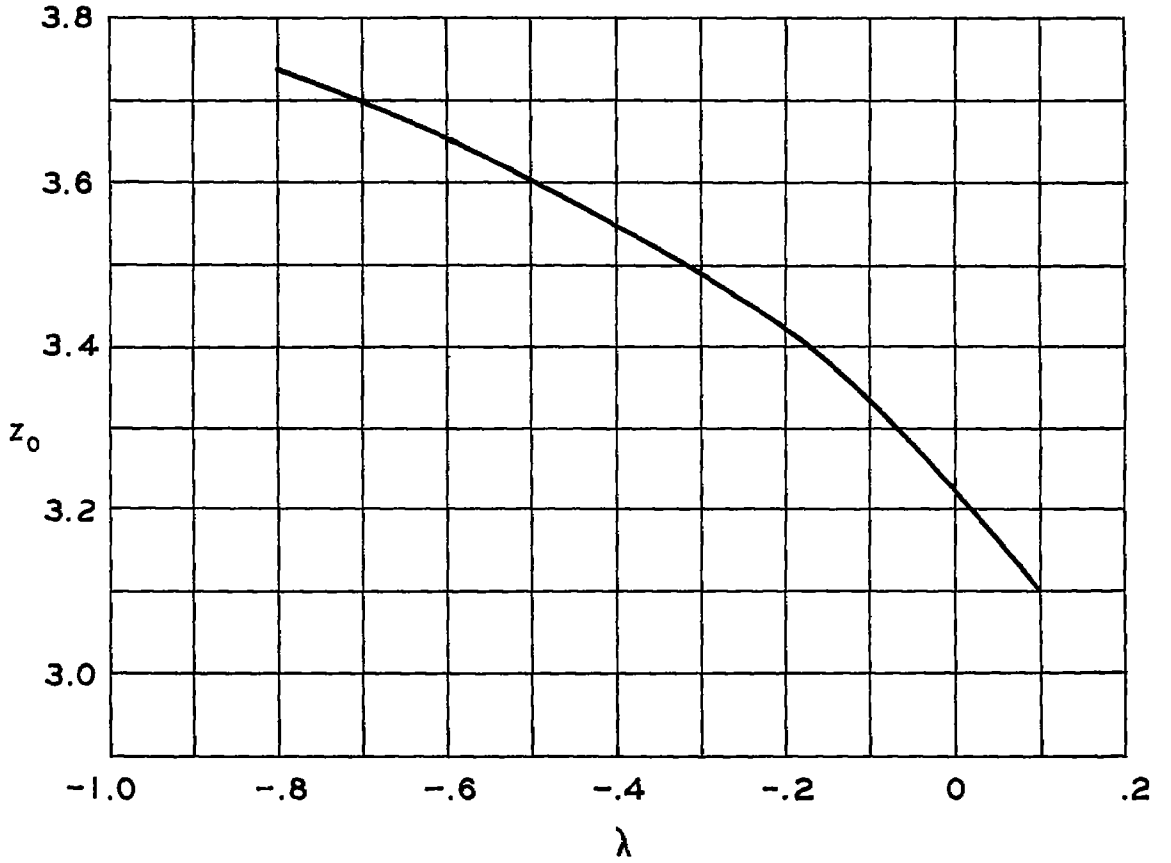

Figure 4.- Plot of z_o as function of λ.

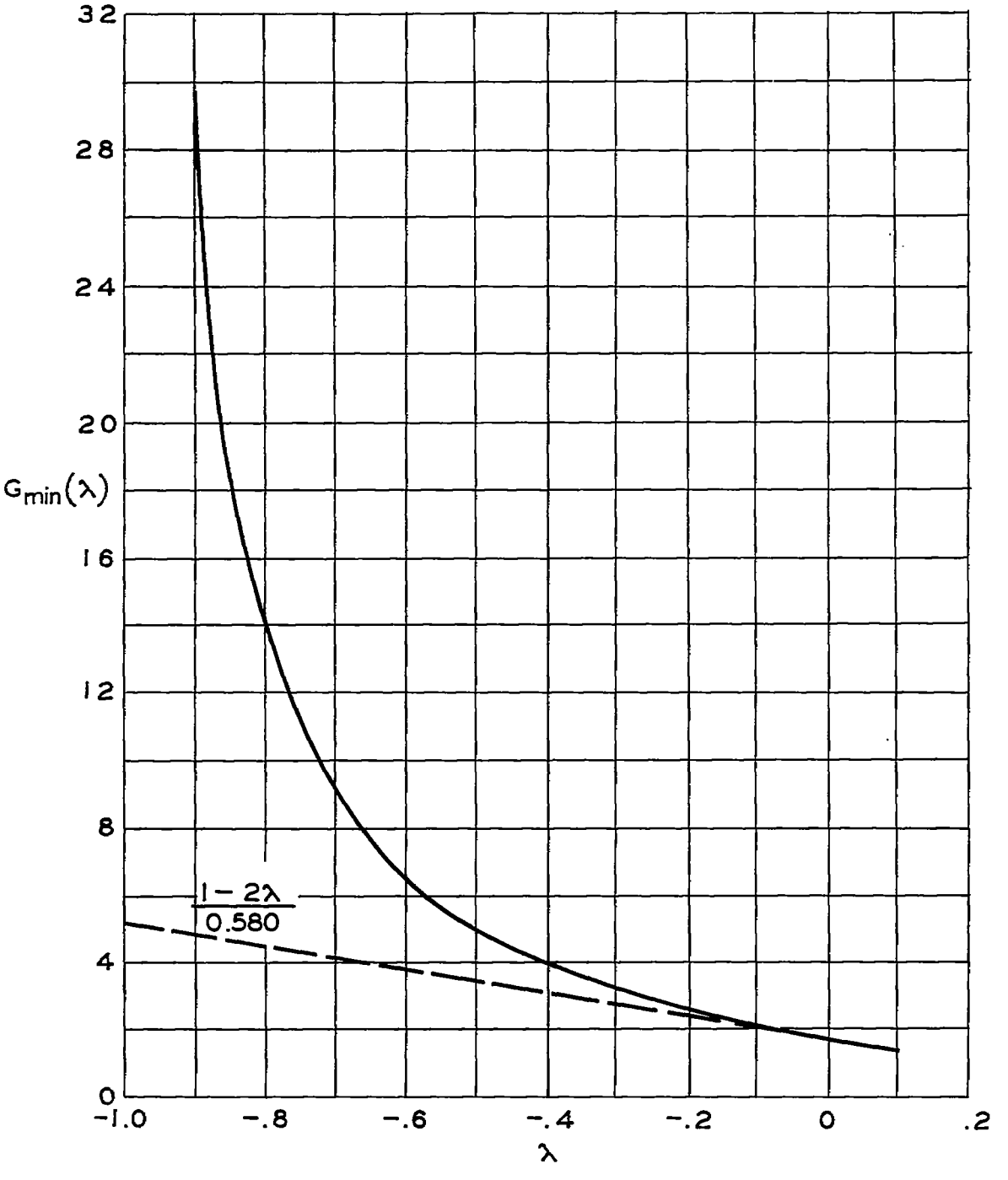

Figure 5.- Minima of $G(z,\lambda)$ with respect to z for fixed values of λ.

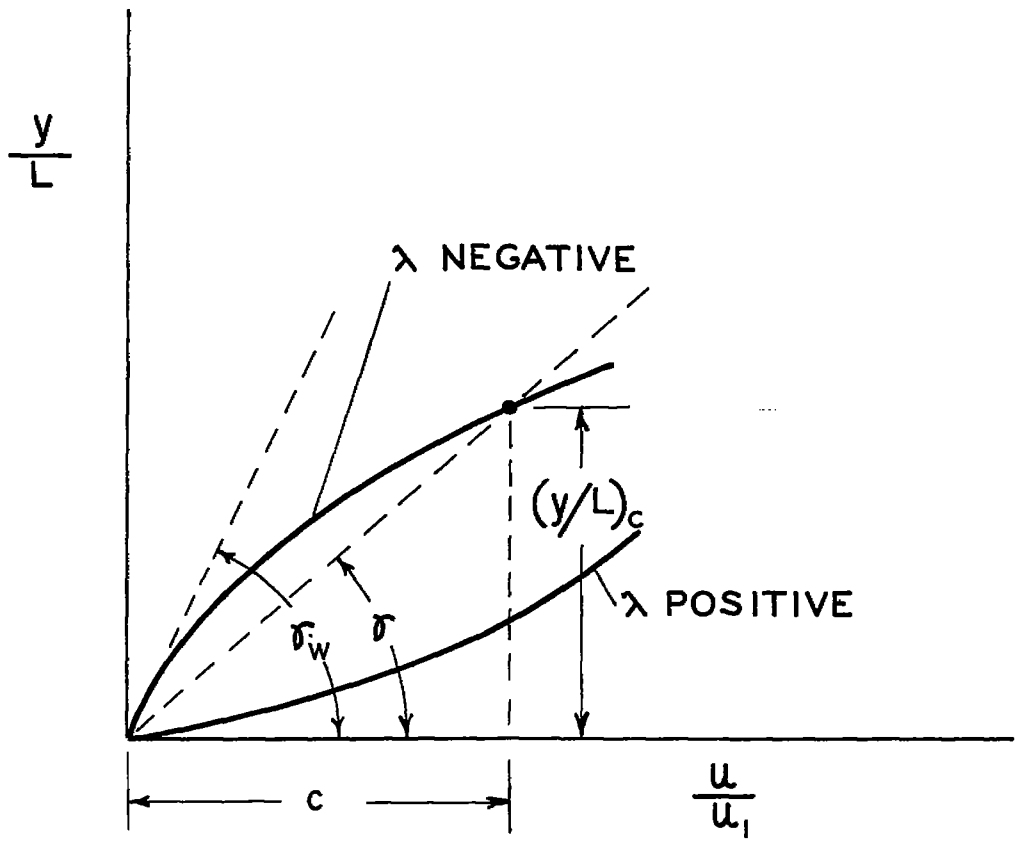

Figure 6.- Geometric significance of boundary-layer profile stability parameter $\lambda(c)$ according to equation (8). $(u/u_1)'_w = 1/\tan \gamma_w$; $(y/L)_c/c = \tan \gamma$; therefore, $\lambda = \frac{\tan \gamma}{\tan \gamma_w} - 1$.

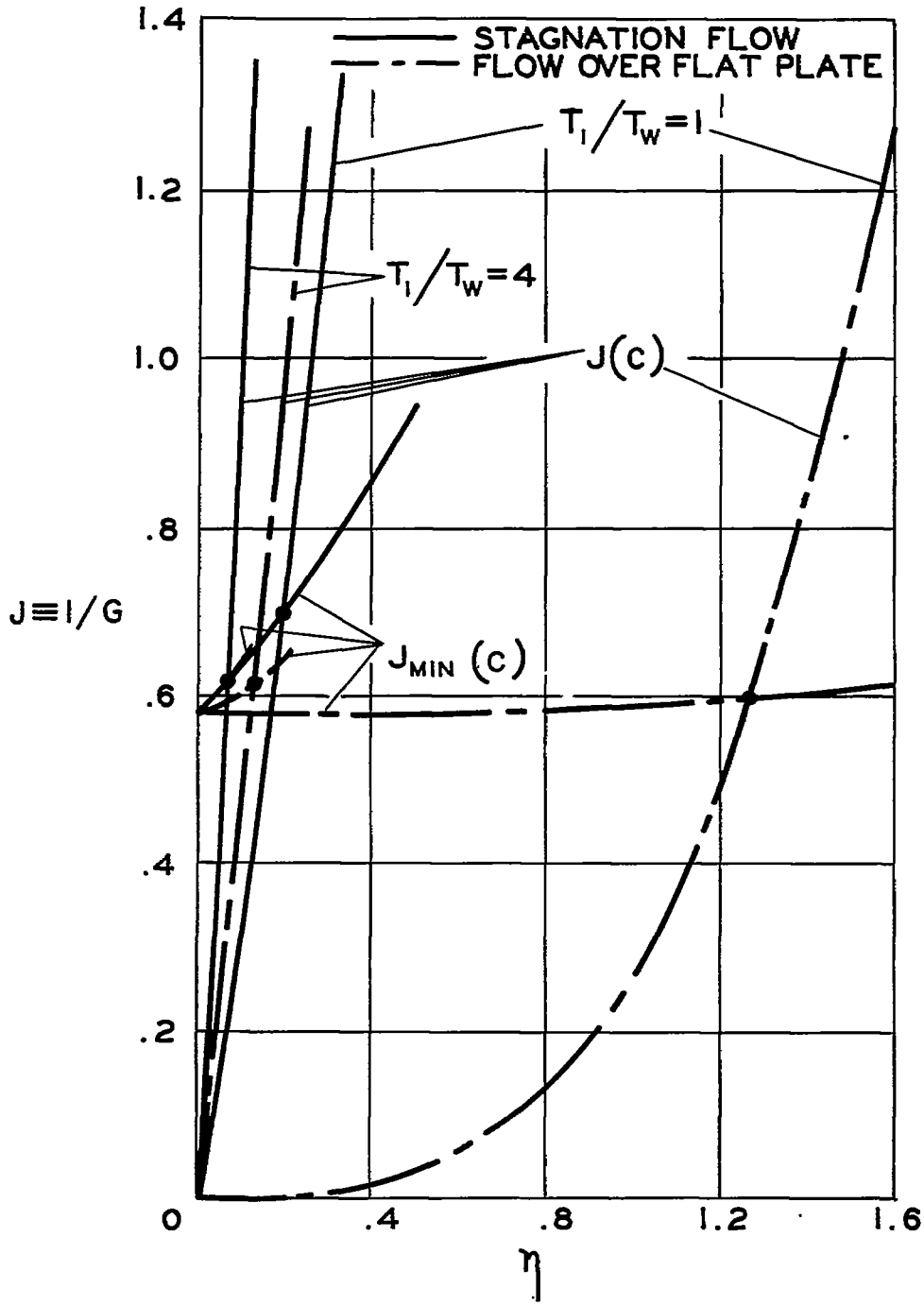

Figure 7.- Determination of c_o for several different cases. $f_w = 0$; dots indicate location of critical layers.

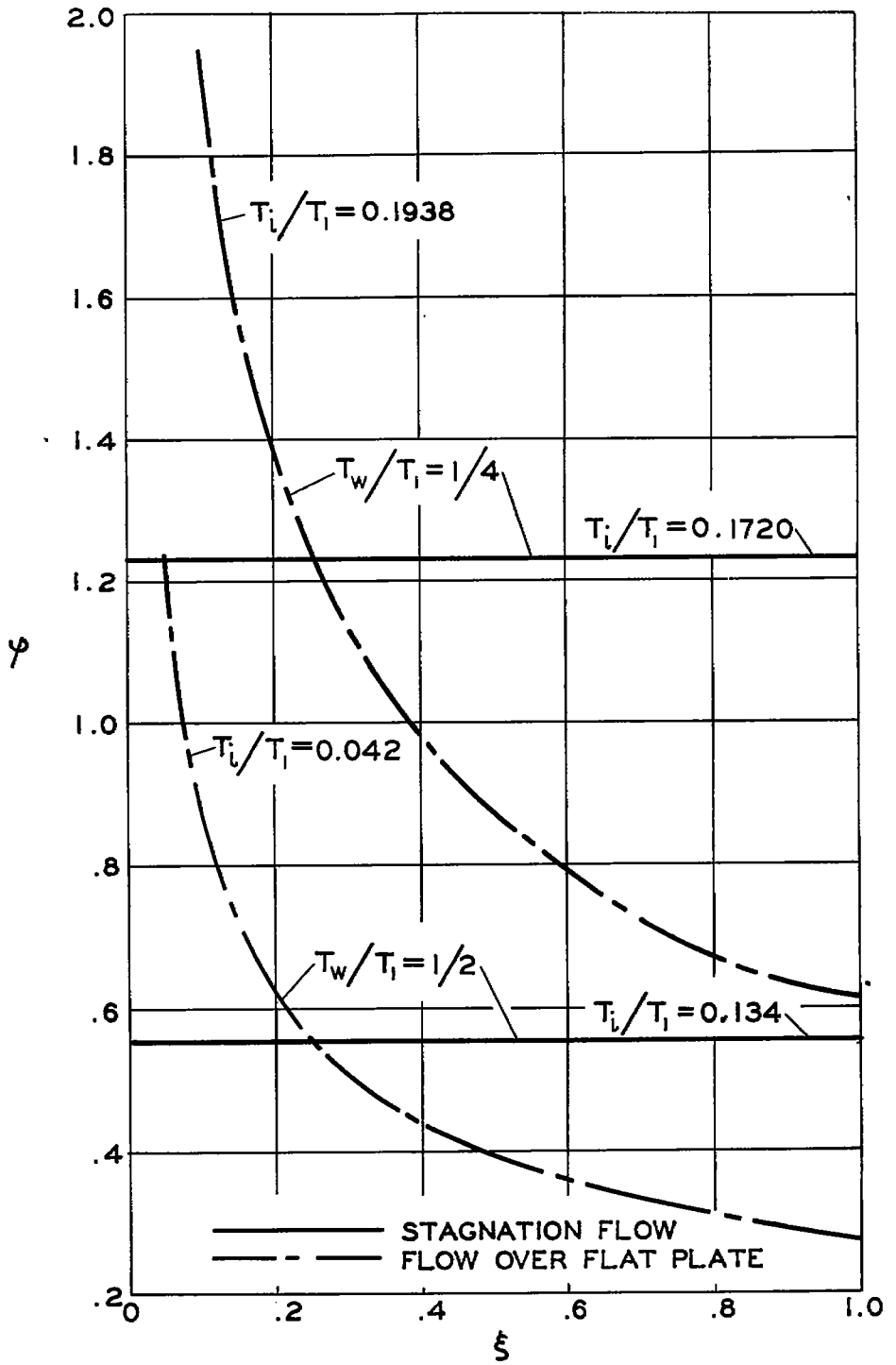

Figure 8.- Distribution of normal mass-flow injection at wall.

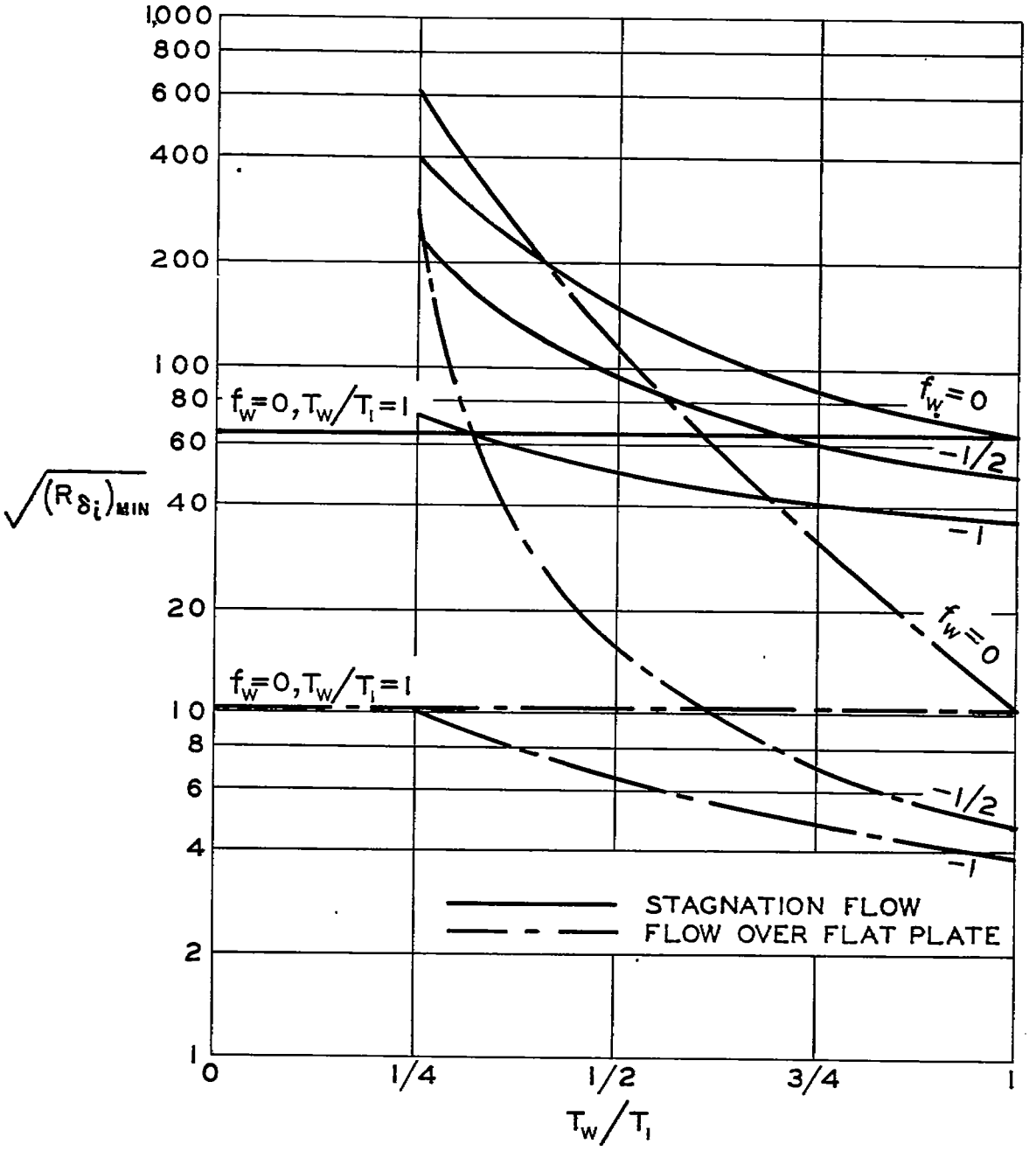

Figure 9.- Minimum critical Reynolds number, based on momentum thickness, as function of wall temperature for various rates of normal fluid injection.

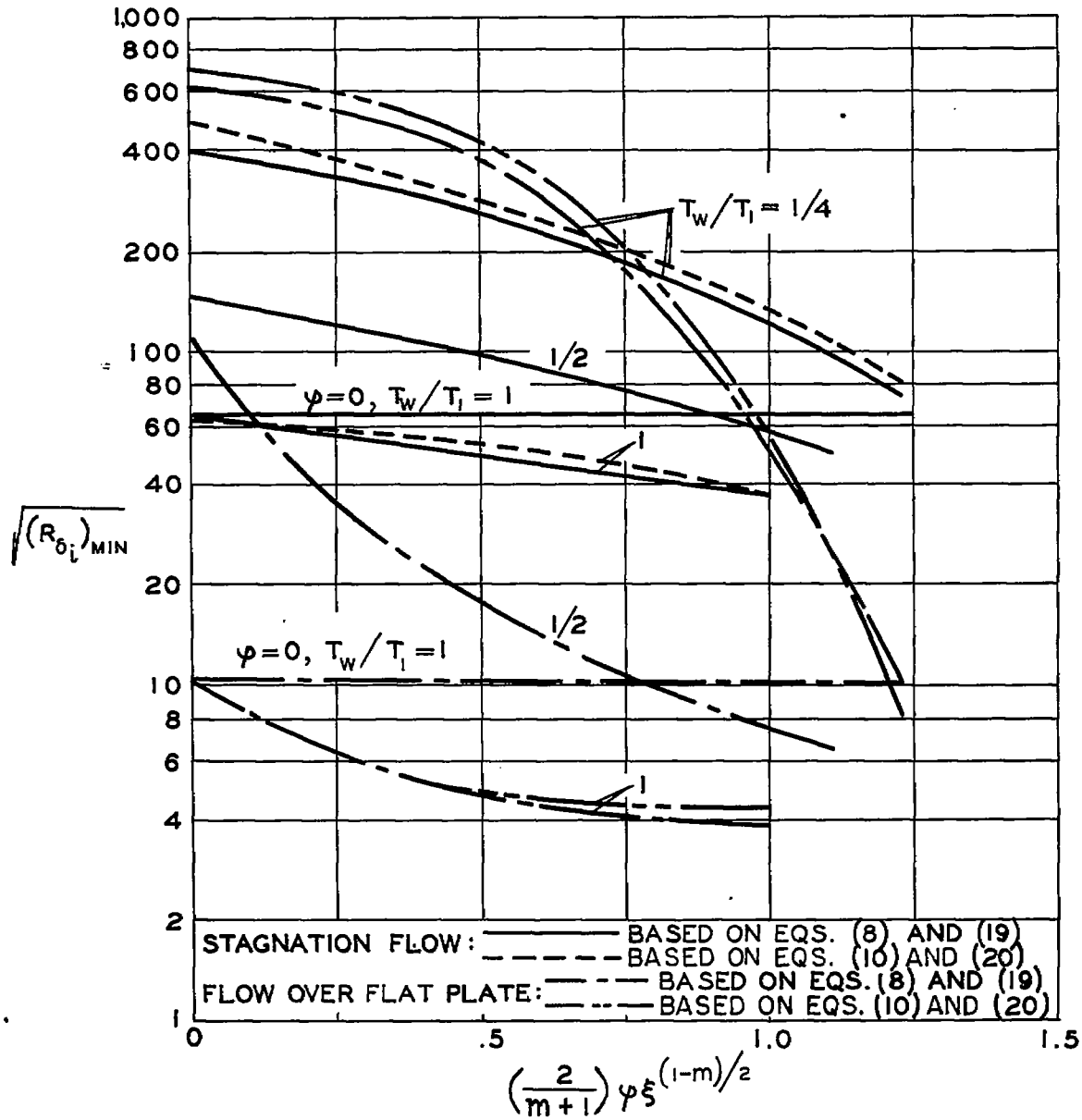

Figure 10.- Minimum critical Reynolds number based on momentum thickness as function of normal fluid injection rate for various wall temperatures.

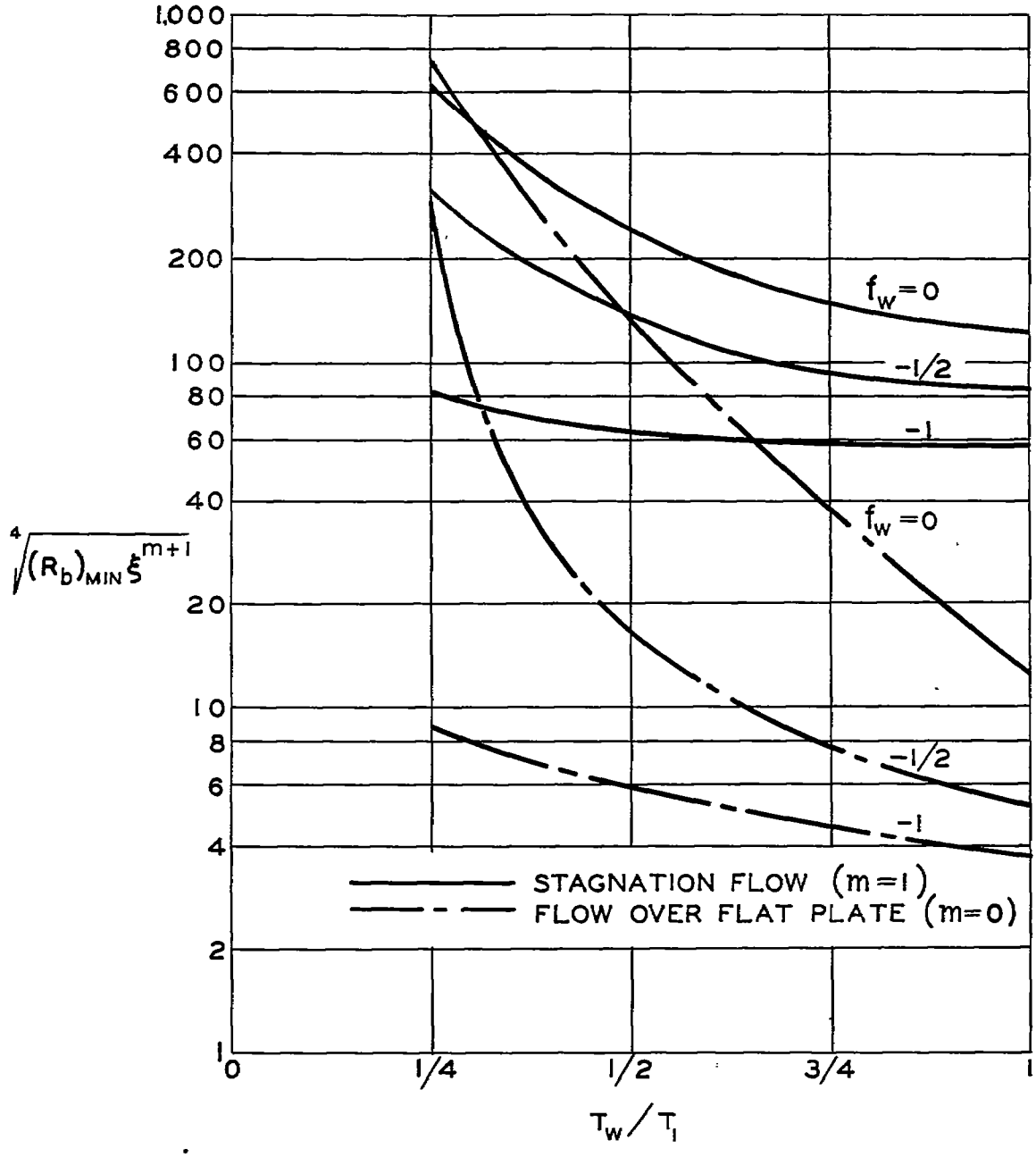

Figure 11.- Minimum critical main-stream Reynolds number as function of wall temperature for various rates of normal fluid injection.

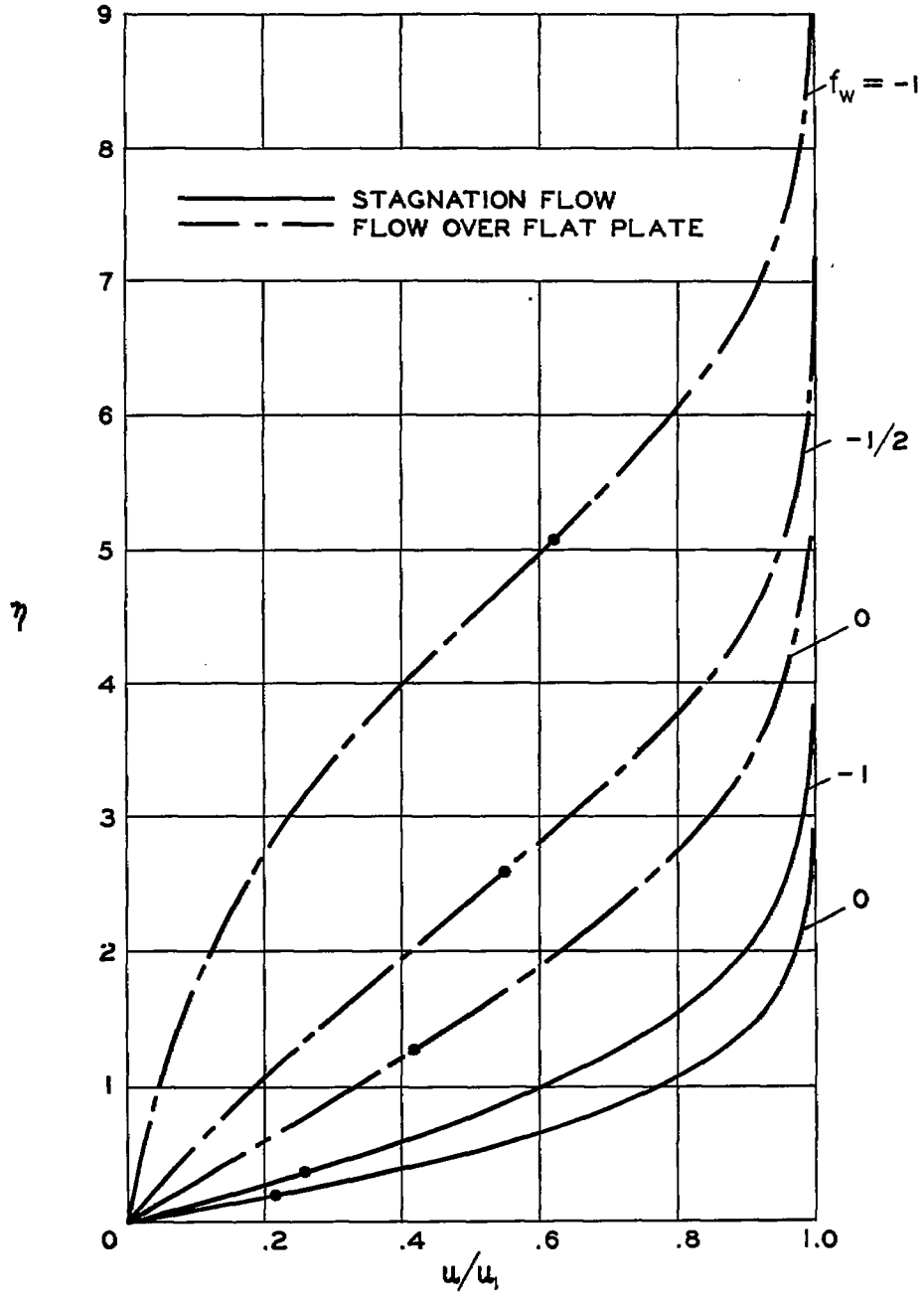

(a) $T_w/T_1 = 1$.

Figure 12.- Velocity profiles (dots indicate location of critical layers).

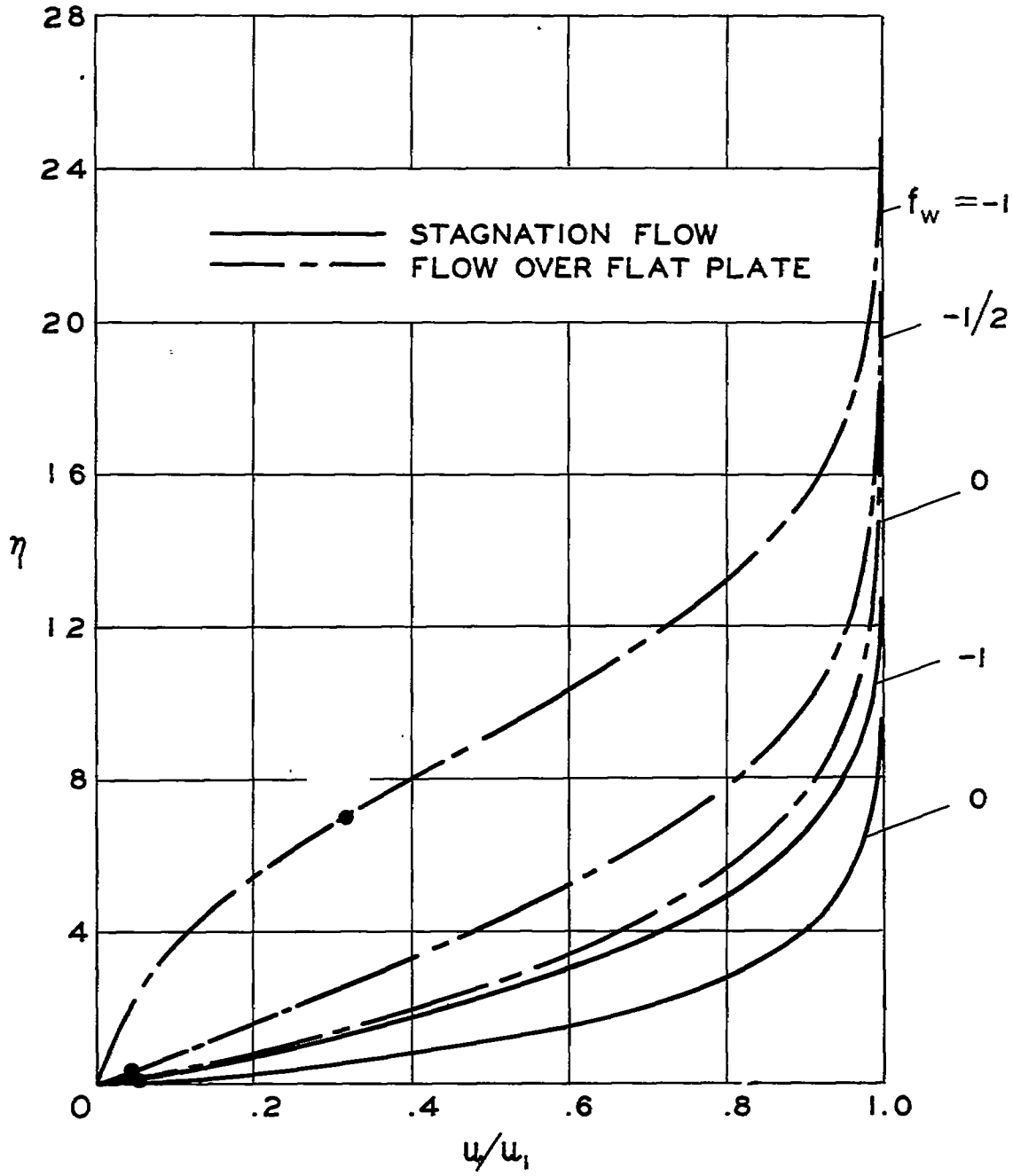

(b) $T_w/T_1 = 1/4$.

Figure 12.- Concluded.

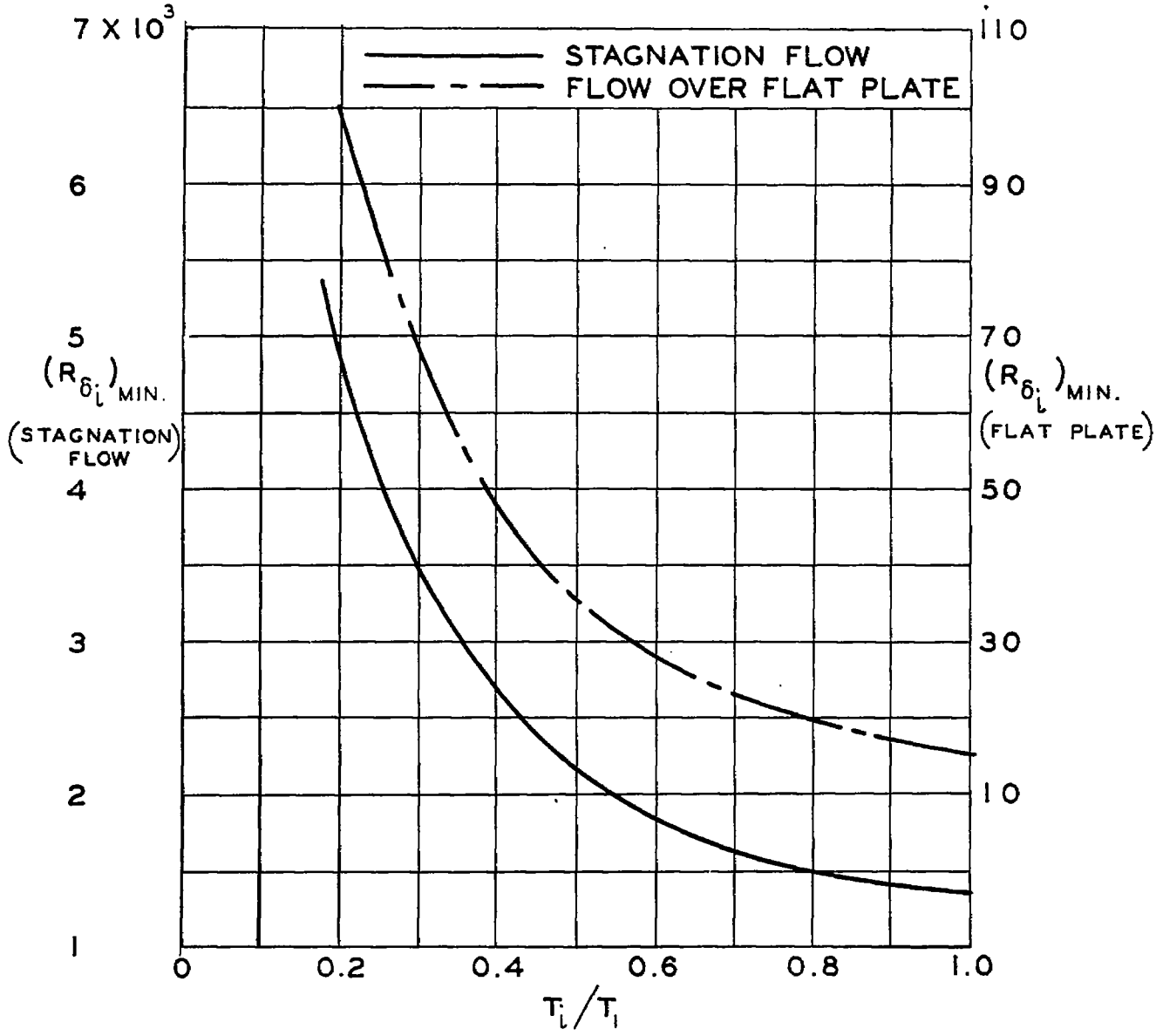

Figure 13.- Minimum critical Reynolds number as function of coolant temperature. $f_w = -1$.